NRDL TRC-68-69

AD

TR - 27

Final Report

EXPERIMENTAL ANALYSIS OF INTERIOR PARTITIONS, APERTURES AND NONUNIFORM WALLS

December 1968

by

J. Velletri, R. Spring
J. Wagoner, H. Gignilliat

For

Office of Civil Defense

Through

U.S. Naval Radiological Defense Laboratory
San Francisco, California 94135

and

Joint Civil Defense Support Group
Office of Chief of Engineers
Department of the Army
Washington, D. C. 20315

Prepared by

CONESCO Division of Flow Corporation
Contract No. DACA 31-67-C-0018
Subtask 1117C

Destroy this report when no longer needed. Do not return it to the originator.

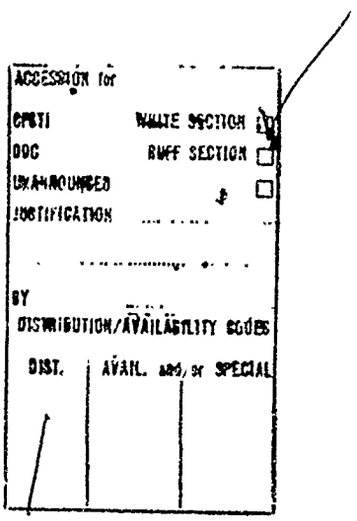

OCD Review Notice

This report has been reviewed in the Office of Civil Defense and approved for publication. Approval does not signify that the contents necessarily reflect the views and policies of the Office of Civil Defense.

DETACHABLE SUMMARY
OF REPORT NO. TR-27
EXPERIMENTAL ANALYSIS OF INTERIOR PARTITIONS, APERTURES AND NONUNIFORM WALLS

December 1968

Technical Report Prepared for

Office of Civil Defense
Office of the Secretary of the Army
Washington, D. C. 20310

Through

The Radiation Test Facility
Joint Civil Defense Support Group
Office of Chief of Engineers
Department of the Army
Washington, D. C. 20315

By

CONESCO, A Division of Flow Corporation
Watertown, Massachusetts
Contract No. DACA 31-67-C-0018
Subtask 1117C

This is a summary of a report which has been reviewed in the Office of Civil Defense and approved for publication. Approval does not signify that the contents necessarily reflect the views and policies of the Office of Civil Defense.

o

DETACHABLE
SUMMARY

The theory of radiation attenuation in complex structures has received much attention during the past few years. The principles have been worked out for application to simple configurations of floors and outside walls so that radiation intensities, within these idealized buildings, from plane fallout fields can be predicted with reasonable accuracy. For other situations, such as a multistory structure having interior partitions, apertures, and nonuniform walls, however, either experimental data do not agree well with computed values or the experimental data usually obtained from existing structures fail to indicate clearly which aspects of the theory require modification.

The purpose of the experimental work reported here was to evaluate systematically the present procedures for estimating the shielding influence of building components in real structures. Experimental data on the effects of interior partitions, apertures, and nonuniform walls in real geometries were obtained by a series of measurements made on the three-story test structure that was previously used in studies at the Radiation Test Facility (RTF). Two typical interior partition configurations were investigated: a box-shaped central core room and a 12-foot-wide corridor forming three rooms within the 24-by-36-foot test structure. In the aperture experiments, the exterior walls of the test structure were altered so that 1/9 of the wall area on the first and second stories consisted of apertures and 1/3 of the wall area on the third story remained open. The exterior walls of the structures for the nonuniform wall experiments consisted of 4-and-8-inch concrete slabs with 1/3 of the wall area occupied by 8-inch slabs.

Each building component was evaluated separately for its shielding influence on the structure. In addition, combinations of these components were investigated.

Major conclusions drawn from this study were:

Interior Partitions

1. For a given total wall thickness, experimental dose rates in the center of the structure increase as the partitions are moved toward the detector.
2. The reduction factors calculated for the structure with interior partitions are between 15 and 20 percent higher than experimental results for detector locations 3 feet above the floors.
3. The experimental reduction factors increase more rapidly with height above the floor than predicted by the calculations.

Apertures

1. The reduction factors calculated for the structure with apertures followed the general trend of the experimental results, but are conservative by as much as 30 percent.
2. The reduction factors calculated for the structure with apertures and interior partitions show the same trend as the experimental values but are less conservative than the results without the interior partitions. In locations below sill height the calculations were slightly nonconservative.

Nonuniform Walls

1. The use of azimuthal sectors in the calculations appears to be valid. The agreement with experiment is about the same as that noticed for experiments with uniform walls.
2. The presence of interior partitions in the structure with nonuniform exterior walls did not appreciably affect the accuracy of the calculational technique.

ooo

TR - 27

FINAL REPORT

EXPERIMENTAL ANALYSIS OF INTERIOR PARTITIONS, APERTURES AND NONUNIFORM WALLS

December 1968

by

J. Velletri, R. Spring
J. Wagoner, H. Gignilliat

For

Office of Civil Defense
Office of the Secretary of the Army
Washington, D. C. 20310

Through

U.S. Naval Radiological Defense Laboratory
San Francisco, California 94135

and

Joint Civil Defense Support Group
Office of Chief of Engineers
Department of the Army
Washington, D. C. 20315

Prepared by CONESCO Division of Flow Corporation
Contract No. DACA 31-67-C-0018
Subtask 1117C

SUMMARY

The theory of radiation attenuation in complex structures has received much attention during the past few years. The principles have been worked out for application to simple configurations of floors and outside walls so that radiation intensities, within these idealized buildings, from plane fallout fields can be predicted with reasonable accuracy. For other situations, such as a multistory structure having interior partitions, apertures, and nonuniform walls, however, either experimental data do not agree well with computed values or the experimental data usually obtained from existing structures fail to indicate clearly which aspects of the theory require modification.

The purpose of the experimental work reported here was to evaluate systematically the present procedures for estimating the shielding influence of building components in real structures. Experimental data on the effects of interior partitions, apertures, and nonuniform walls in real geometries were obtained by a series of measurements made on the three-story test structure that was previously used in studies at the Radiation Test Facility (RTF). Two typical interior partition configurations were investigated: a box-shaped central core room and a 12-foot-wide corridor forming three rooms within the 24-by-36-foot test structure. In the aperture experiments, the exterior walls of the test structure were altered so that 1/9 of the wall area on the first and second stories consisted of apertures and 1/3 of the wall area on the third story remained open. The exterior walls of the structures for the nonuniform wall experiments consisted of 4-and-8-inch concrete slabs with 1/3 of the wall area occupied by 8-inch slabs.

Each building component was evaluated separately for its shielding influence on the structure. In addition, combinations of these components were investigated.

Major conclusions drawn from this study were:

Interior Partitions

1. For a given total wall thickness, experimental dose rates in the center of the structure increase as the partitions are moved toward the detector.
2. The reduction factors calculated for the structure with interior partitions are between 15 and 20 percent higher than experimental results for detector locations 3 feet above the floors.
3. The experimental reduction factors increase more rapidly with height above the floor than predicted by the calculations.

Apertures

1. The reduction factors calculated for the structure with apertures followed the general trend of the experimental results, but are conservative by as much as 30 percent.
2. The reduction factors calculated for the structure with apertures and interior partitions show the same trend as the experimental values but are less conservative than the results without the interior partitions. In locations below sill height the calculations were slightly nonconservative.

Nonuniform Walls

1. The use of azimuthal sectors in the calculations appears to be valid. The agreement with experiment is about the same as that noticed for experiments with uniform walls.
2. The presence of interior partitions in the structure with nonuniform exterior walls did not appreciably affect the accuracy of the calculational technique.

FOREWORD

The experiments described in this report were performed in the period of July 1966 through January 1968 by the CONESCO Division of Flow Corporation, Watertown, Massachusetts at the Radiation Test Facility, Fort Belvoir, Virginia.

This work was conducted for the Office of Civil Defense through the RTF, Joint Civil Defense Support Group (JCDSG), Office of the Chief of Engineers under Contract No. DACA 31-67-C-0018 Subtask 1117C.

The authors are indebted to Mr. Steven Horne and Mr. John Musala, of CONESCO, for their efforts in the performance of the experiments and to Mr. Charles Eisenhauer of the National Bureau of Standards, Mr. H. Wheeler of JCDSG, and Mr. John LeDoux of CONESCO for their helpful suggestions and criticisms.

TABLE OF CONTENTS

LIST OF ILLUSTRATIONS

LIST OF ILLUSTRATIONS

LIST OF TABLES

NOMENCLATURE

A_Z	=	azimuthal section ratio
$B_e(X_e, h)$	=	attenuation introduced by a vertical wall to an infinite field of contamination
$B_{ws}(X_e, \omega_s)$	=	attenuation introduced by a vertical wall to a finite field of contamination
$B_o'(X_o')$	=	attenuation introduced by a horizontal barrier to "in-and-down" scattered radiation
$B_o'(X_f, \varpi)$	=	modified values of the attenuation introduced by a horizontal barrier to "in-and-down" scattered radiation
$B_f(X_f)$	=	attenuation introduced by a horizontal barrier to "in-and-up" scattered radiation
$B(\mu x)$	=	dose buildup factor
D	=	dose rate
D_o	=	infinite field dose rate at 3 feet above a smooth plane
E	=	eccentricity factor for the structure
$G_d(\omega)$	=	cumulative angular distribution of direct radiation
$G_s(\omega)$	=	cumulative angular distribution of scattered radiation
$G_a^*(\omega)$	=	cumulative angular distribution of skyshine radiation
$G_a(\omega)$	=	cumulative angular distribution of skyshine plus ceiling shine radiation
h, d or x	=	detector height in ft, or equivalent mass thickness
L(X)	=	functional attenuation of the dose above an infinite field source covered with an attenuating mass of thickness X

$\ell(d, \cos\theta)$	=	angular distribution of radiation in an air-over-ground infinite field case
$S_a(d, \omega)$	=	skyshine angular distribution
$S'(X)$ or $S'(d)$	=	skyshine attenuation function
$S_w(X_e)$	=	fraction of radiation scattered by a vertical wall
$W(X, d)$	=	attenuation introduced by a vertical wall normalized to 0.5
X_e	=	vertical wall thickness in pounds per square foot (psf)
X_o	=	basement ceiling thickness (psf)
X_f	=	floor thickness (psf)
θ	=	angle between an axis perpendicular to the plane of contamination and the direction of interest
ω	=	solid-angle fraction (the solid angle divided by 2π)
$\overline{\omega}$	=	average solid-angle fraction
ω_ℓ	=	solid-angle fraction of the floor immediately below the detector
ω_ℓ'	=	solid-angle fraction of the floor two floors below the detector
ω_U	=	solid-angle fraction of the floor immediately above the detector
ω_U'	=	solid-angle fraction of the floor two floors above the detector
ω^*	=	solid-angle fraction of finite field as observed from detector
ω_s	=	solid-angle fraction of finite field as observed from mid-wall position
W_c	=	width of contaminated area, from base of structure ft.

R	=	radius of contaminated area from face of structure, ft.
X_i	=	interior partition thickness (psf)
ω_a	=	solid angle fraction of top of aperture
ω_a'	=	solid angle fraction of sill of aperture
P_a	=	perimeter ratio
A_p	=	aperture percentage
$B_i\ (X_i)$	=	interior partition barrier factor

CHAPTER 1

INTRODUCTION

The theory of radiation attenuation in complex structures has received much attention during the past few years. The principles have been worked out for application to simple configurations of floors and outside walls so that radiation intensities, within these idealized buildings, from plane fallout fields can be predicted with reasonable accuracy. For other situations, such as a multistory structure having interior partitions, apertures, and nonuniform walls, however, either experimental data do not agree well with computed values or the experimental data usually obtained from existing structures fail to indicate clearly which aspects of the theory require modification.

In complexity, existing structures may be divided into two groups. These are small buildings such as homes and one-story commerical buildings, and large, multistory, complex structures. Experimental tests have been conducted on typical small structures[1] at the AEC Nevada Test Site and large complex structures[2] in other parts of the United States to determine the accuracy with which shielding factors may be calculated. The experimental work was usually done on complex structures with sloping roofs, inhomogeneous barrier materials, and in many cases unknown barrier density, so that the results were not directly comparable with theory.

The purpose of the experimental work reported here was to evaluate systematically the present procedures[3] for estimating the shielding influence of building components in real structures. Experimental data on the effects of interior partitions, apertures, and nonuniform walls in real geometries were obtained by a series of measurements on the three-story test structure that had been used in previous studies[4, 5, 6, 7] at the Radiation Test Facility (RTF). Two typical interior partition configurations were investigated: a box-shaped central core room, and a 12-foot-wide corridor forming three rooms within the 24-by-36-foot test structure. In the aperture experiments, the exterior walls of the test structure were altered so that 1/9 of the wall area on the first and second stories consisted of apertures and 1/3 of the wall area on the third story remained open. The exterior walls of the structures for the nonuniform wall experiments consisted of 4- and 8-inch concrete slabs, with 1/3 of the wall area occupied by 8-inch slabs.

Each building component was evaluated separately for its shielding influence on the structure. In addition, combinations of these components were investigated.

CHAPTER 2

EXPERIMENTAL ARRANGEMENT AND TECHNIQUE

The experiments described in this study were conducted on the three-story test structure at the Radiation Test Facility, Fort Belvoir, Virginia. The method of obtaining a simulated field of radioactive contamination and the experimental test structure have been described in previous reports.[4, 5, 6] The basic structure is briefly described here and modifications to the basic building are described in the appropriate sections.

2.1 TEST STRUCTURE

The radiation test structure consists of a steel skeleton (Fig. 2.1) with internal dimensions of 24 by 36 feet at the base, and 36 feet high, with provision for floors (or ceilings) at the 11-,23-,and 35-foot elevations, and with a basement 6 feet in depth. The exterior building columns are 14 B 26 wide - flange beams which extend the height of the building. A grid of 8-inch wide-flange beams 12 feet in length spaced 4 feet on center, are located 11, 23, and 35 feet above the ground.

The structure can be made to represent a variety of building configurations by assembling concrete panels (each 4 feet by 4 feet by 4 inches thick) into the desired modular design. The design allows walls and floors to be varied conveniently in thickness from 0 to 12 inches in 4-inch increments. The walls and floors of the test structure for the experiments described in this report were 4 and 8 inches thick respectively.

2.2 SIMULATED FALLOUT FIELD

The simulated field of contamination (the design of which is described in detail in Ref. 4) consisted of a quadrant of a circle of 452-foot radius, concentric with the test structure, which was divided into four annular test areas (Fig. 2.2). Since the structure exhibited quarter symmetry, only one quadrant of the field had to be simulated; hence, the summation of dose rates of symmetrically located detectors provided results equivalent to those which would have been obtained if the full field had been simulated. The contaminated field was simulated by pumping sealed Co-60 sources at constant velocity through a network of tubing that occupied each of four annular areas of the quadrant. The infinite field dose is approximated by the sum of the dosage received by the detector from each of the four areas, plus an estimated contribution, based on the outermost simulated area to represent "far-field" sources of contamination. This estimate is based on the assumption that the attenuation of radiation by the structure is the same for the last measured annulus as for the far-field. The far-field generally represents approximately 10 percent of the total dosage, so that any inaccuracy introduced by this assumption would be small. This method of estimate is described in detail in Reference 4.

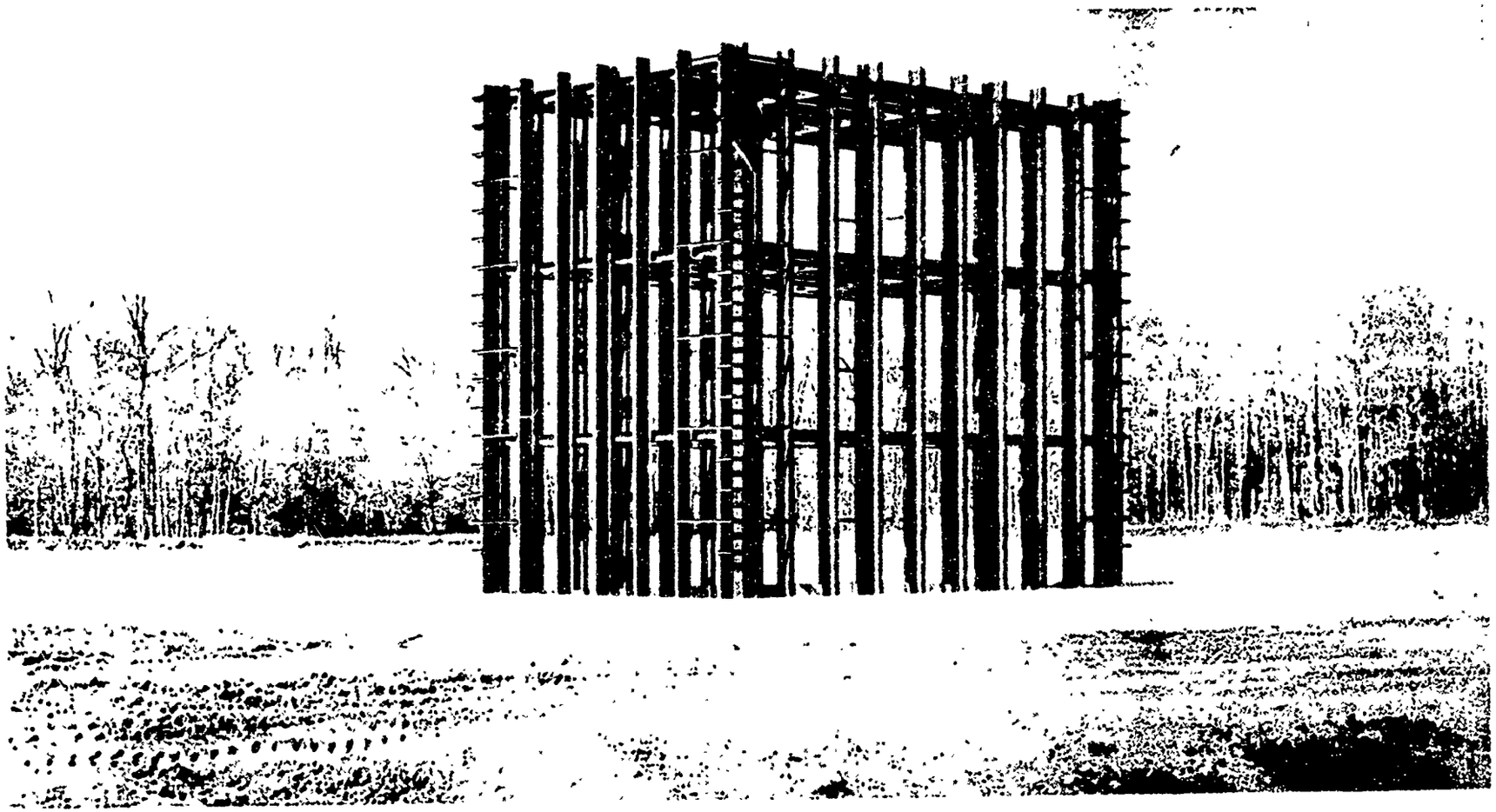

Figure 2.1 Steel Frame of Test Structure

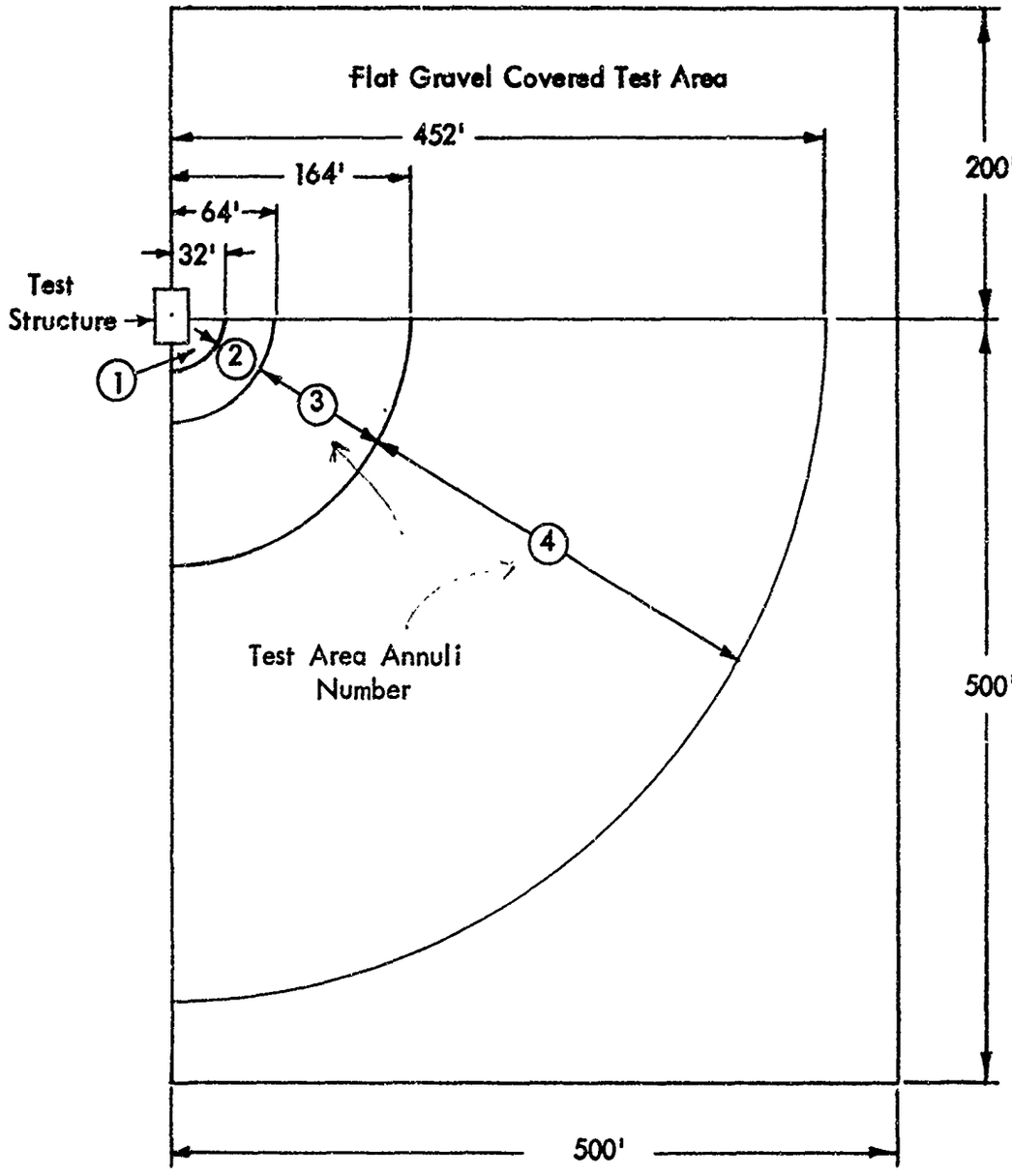

Plan View of Test Area

Figure 2.2

2.3 EXPERIMENTAL TECHNIQUE

The experimental technique consisted of measuring the radiation dose at points within the building from a simulated area of contamination of known strength outside the building. Data were obtained by means of air core capacitor ionization chambers of 200-, 10-, or 1-mR capacity together with a "charger-reader" that functioned by measuring the total integrated current required to return a capacitor to its original voltage after exposure in the radiation field. Chamber (capacity) selection was based on the exposure time, the section of the field being simulated, the thickness of the walls and floors, and the locations of the test positions with respect to the contaminated area.

Before this experiment was begun, all ionization chambers and the charger-reader were calibrated against a gamma source of known strength and a National Bureau of Standards calibrated Victoreen R meter. All the chambers selected for use in the experiment responded to within ± 2 percent of the known dose. The chambers were also checked at intervals during the experiment by a secondary calibration procedure.

Dose measurements were taken within the test structure in each structure configuration investigated. Detector positions were generally arranged in a vertical array. Throughout this report the specific location of a detector is referred to as its X, Y coordinates in relation to the centerline of the structure. Height was measured either from the ground or, if floors were in place, from the upper surface of the floor immediately below the detector. Note: the simulated quarter field of contamination is located in the plus X minus Y quadrant (Fig. 2.3).

2.4 NORMALIZATION AND ACCURACY OF EXPERIMENTAL DATA

All detector readings were normalized to a specific dose rate; that is, to a per hour basis for an equivalent contamination density of 1 curie of Co-60 per square foot. This is the source density that produced a radiation field of 464 R/hr 3 feet above an infinite, smooth, uniformly contaminated plane in an earlier experiment[4] conducted at the Radiation Test Facility (see Appendix A). Detector readings were converted to R/hr using chamber calibration constants, exposure time, source strength, and temperature-pressure corrections for the effect of atmospheric conditions. The normalization is described in detail in Reference 4. Data tables for these experiments are presented in Appendix A.

To determine the accuracy of the data obtained from these experiments, the errors or uncertainties of many parameters must be considered. Since it was impractical to determine experimentally in a completely rigorous way all the variables associated with weather, exposure time, source strength, and so forth, it was necessary to estimate some of the errors and uncertainties from practical experience. A detailed analysis of those errors is presented in Appendix C of Reference 7. Compounding these uncertainties according to accepted principles, we find that the estimated standard deviation in the specific dose rate is 3 percent and, in the infinite field reduction factor, 4 percent.

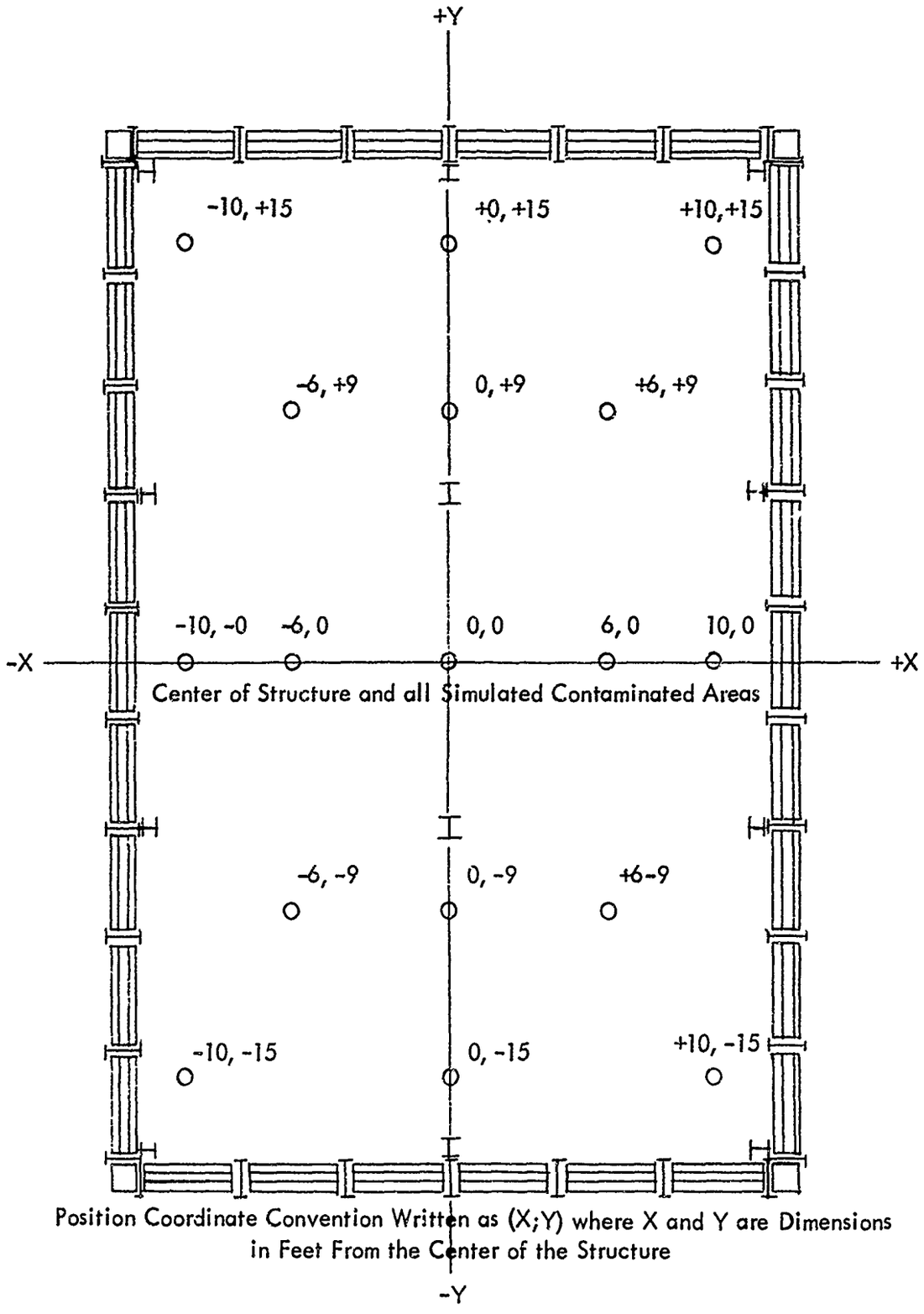

Figure 2.3 Sketch of Coordinate Convention in Test Structure

BLANK PAGE

CHAPTER 3

STRUCTURE WITH INTERIOR PARTITIONS

The presence of multiple barriers in structural design may strongly influence the reduction factors in shelter areas. The additional barriers are usually interior partitions either parallel to or perpendicular to the exterior walls or a combination of both. The theoretical method used for structure shielding calculations[3] provides a simple technique to account for interior partitions. The experiments described in this section were designed to evaluate this technique.

3.1 THEORY

The method currently used for estimating the effects of interior partitions on the dose rates in a structure as described in Reference 3 is based on the assumption that when interior partitions are present, reduction in intensity is due solely to barrier reduction. Although such a partition affects both the geometry and the barrier reduction factors, only the barrier effects are considered in the current method. Geometry effects are ignored in the calculations partly because of the uncertainty of these effects and partly because of the complications they introduce into the method.

The procedure for taking into account the ground contribution passing through parallel (to the exterior wall) partitions (Fig. 3.1a) requires calculations that assume no interior partitions and then further reduction by a barrier factor which is a function of the mass thickness of the interior wall. The barrier factor for the interior wall is assumed to be independent of height, because a height correction is included in the barrier factor for the exterior wall.

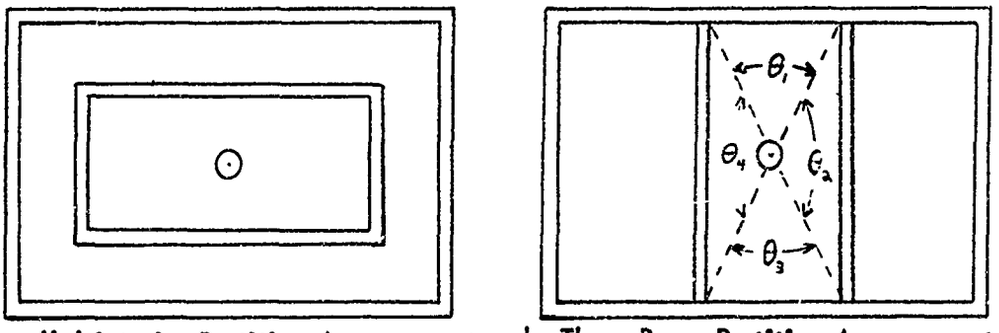

a. Parallel Interior Partition Arrangement b. Three Room Partition Arrangement

Figure 3.1 - Partition Arrangement

In the Engineering Method[3] terminology, the reduction factor for ground contribution of infinite extent in a single story structure without interior partitions is:

$$D/D_o = \left\{ \left[G_d(\omega_\ell, h) + G_a(\omega_U) \right] \left[1-S_w \right] + \left[G_s(\omega_U) + G_s(\omega_\ell) \right] S_w(X_e) E \right\} B_e(X_e, h) \qquad (3.1)$$

where

$G_d(\omega)$	=	cumulative angular distribution of direct radiation
$G_a(\omega)$	=	cumulative angular distribution of atmospheric-scattered radiation
$G_s(\omega)$	=	cumulative angular distribution of wall scattered radiation
ω	=	solid-angle fraction (solid angle / 2π)
S_w	=	fraction of emergent radiation scattered in wall barrier
E	=	shape factor
h	=	detector height
$B_e(X_e, h)$	=	barrier shielding introduced by a vertical wall thickness X_e at height h above ground

and in the center of the structure having parallel interior partitions:

$$RF = RF^* \times B_i(X_i, 3') \qquad (3.2)$$

where:

RF^*	=	reduction factor in structure without interior partitions
$B_i(X_i, 3')$	=	barrier factor for interior partitions (Reference 3, Case 2, Chart 1)

In the event that an interior partition arrangement does not surround the detector location (as illustrated in Fig. 3.1b), the structure is analyzed using azimuthal sectors about the detector. The contribution from each sector is determined and the results are summed to obtain the total contribution.

To analyze the configuration shown in Fig. 3.1b two sectors are required: one comprised of the mass thickness of the exterior wall, A_{Z1} and the other of the mass thickness of the exterior wall plus interior wall, A_{Z2}. The sector angles subtended at a centrally located detector are shown in Fig. 3.1b. Thus the fraction of radiation which reaches the detector without penetrating the interior partition is given by Equation 3.3. Likewise, the fraction that reaches the detector after penetrating the partition is given by Equation 3.4.

$$A_{Z1} = \frac{\theta 1 + \theta 3}{360} \tag{3.3}$$

$$A_{Z2} = \frac{\theta 2 + \theta 4}{360} \tag{3.4}$$

The functional expression for the ground contribution to a centrally located detector then becomes:

$$D/D_o = \left[A_{Z1} + A_{Z2}\ B_i(X_i)\right]\left\{\left[G_d(\omega_\ell, H) + G_a(\omega_u)\right]\left[1-S_w\right] + \left[G_s(\omega_\ell) + G_s(\omega_u)\right] S_w E\right\}\left[B_e(X_e, H)\right] \tag{3.5}$$

Notice that, in Equation 3.5, only the portion of the ground contribution which passes through the partition is multiplied by the interior partition barrier factor, $B_i(X_i)$.

3.2 DESCRIPTION OF STRUCTURE

Two typical interior partition configurations were investigated in this study. The first, designated Configuration A, consisted of a box-shaped central core room in which each interior partition was parallel to a corresponding exterior wall. The partitions extended from the floor to the ceiling on all three stories of the basic test structure. The partitions were constructed of 4-by 8-by 16-inch solid concrete block. The effective mass thickness of the concrete wall was measured as 42 psf. The exterior walls and floors of the basic test structure (see section 2.1) were 49 and 97.2 psf respectively. Two cases of Configuration A were tested. In the first, the central core enclosed by the partitions was 28 by 16 feet, with each interior wall approximately 4 feet from its corresponding ex-

terior wall (see drawing in Fig. 3.3). The interior partitions in the second case formed a 3-by 3-foot core shelter in the center of the test structure.

In Configuration B the interior partitions were parallel to the short side of the rectangular structure and perpendicular to the long side (see drawing in Fig. 3.6). This arrangement divides the 36-by 24-foot test structure into three rooms of plan dimension 24 by 12 feet.

3.3 RESULTS AND ANALYSIS

The effect of interior partitions, as discussed in section 3.1 of this chapter, may be regarded from the standpoint of the calculations as a correction factor applied to the building shell with no interior partitions. The basic structure without interior partitions is described in detail in Reference 7. However, since this structure is so important in this experiment, we will briefly describe that experiment and its results. The vertical dose distributions at the center of the test structure with 97.2-psf floors and 49- and 98-psf walls are reproduced from Reference 7 in Figure 3.2. The experimental results are in the form of reduction factors. The theoretical results shown in this figure were calculated by using Equation 3.1 of this report and Equations 3.5 and 3.6 from Reference 6. The solid line shown in this figure represents theoretical values based on geometry and barrier factors calculated from the basic data of NBS-42[8]. The dashed line represents calculated values in which an experimentally determined barrier factor, $B_e(X_e, \omega)$, was substituted in Equation 3.1 for the calculated barrier factor. The experimental barrier factors are the results of work previously conducted[5] at the RTF, in which the attenuation introduced by a vertical wall up to a height of 33 feet from an infinite field of ground contamination was measured for 49-, 98-, and 147-psf walls. Results of this experiment showed the theoretical barrier factor to be conservative by 12, 18, and 25 percent for the 49-, 98-, and 147-psf barriers, respectively.

Figure 3.2 indicates that better agreement between theoretical and experimental values of reduction factors is achieved when the experimentally determined barrier factor is used in the calculations. However, the experimental reduction factors increase more rapidly with height above floor than predicted by the calculations. It is inferred that the scattered radiation emerging from the walls, G_s, may not by symmetrical with respect to the horizontal, as had been assumed, but may be more peaked in the upward direction. The effect of this asymmetry has been noticed in past experiments[7] and is evident in all the experiments investigated in this study. It suggests that the geometry curve for wall scattered radiation from the lower hemisphere should be different from that for the upper hemisphere. Unfortunately, it was not possible to separate the effect of wall scattered from nonwall scattered radiation in this experiment.

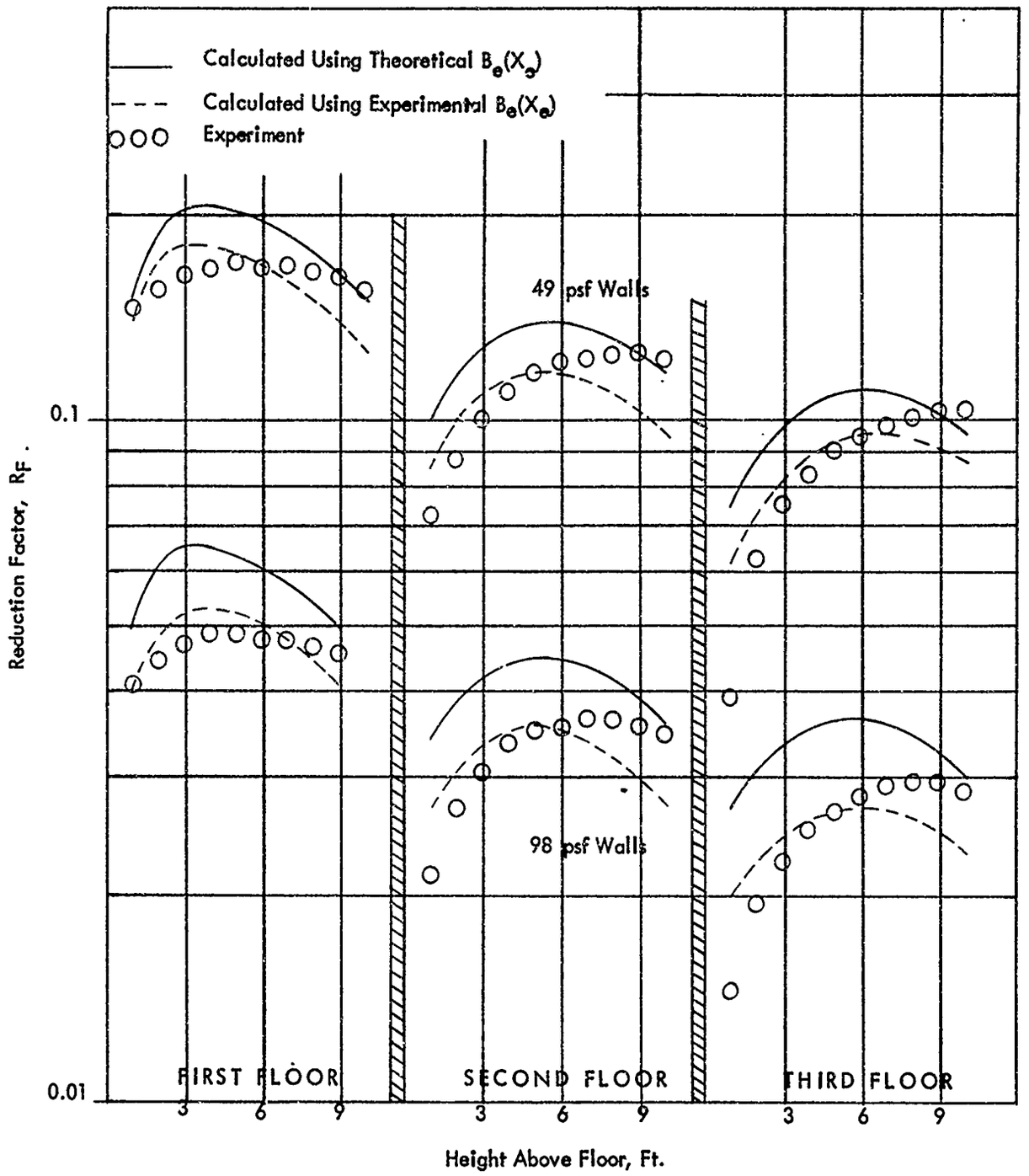

Figure 3.2 - Vertical Dose Distribution at the Center of a Three Story Structure of 24 by 36 Foot Plan Area with 97.2 psf Floors

If it can be assumed that interior partition walls attenuate radiation only as a barrier, the experimental results in the aforementioned experiment should be identical to the experiments conducted on Configuration A of this report. As specified, the wall panels that make up the exterior wall are 49 psf thick whereas the concrete blocks that make up the interior walls are 42 psf thick. Thus, in the experiment without interior partitions, the mass thickness between source and detector was 98 psf, whereas, with interior partitions, the total mass between source and detector was 91 psf. This difference in barrier mass thickness could amount to a 15 percent difference in reduction factors. Any direct comparison between the two experiments would involve an adjustment for barrier mass either in the experimental or the calculated values. However, a direct comparison can be made between the two cases tested in Configuration A. Here the mass thickness between source and detector was 91 psf in both cases. According to the Engineering Method, the dose rate is not dependent on the location of the partition with respect to the detector.

The experimental results for these two cases are present in Table 3.1 and shown in Fig. 3.3, along with the calculated results. The dose distribution as a function of the height above floors appears to have the same general characteristics as that in the structure without interior partitions (Fig. 3.2).

Figure 3.3 indicates that the position of an interior partition in a structure in relation to a detector does affect the dose rate. As the partition is moved toward the detector, the dose rate increases. This increase was approximately 18 percent when the partitions were moved from their position in case 1 to a location 3 feet from the detector (case 2). The calculational procedure provides an interior partition barrier factor, $B_i(X_i, 3')$, which is independent of barrier position — i.e., regardless of the partition's position within the structure, a single value of $B_i(X_i, 3')$, which is a function of the mass thickness of the interior barrier at 3 feet above ground, is used in the calculation.

To minimize the effect of the slight variation in mass thickness between the structure without interior partitions (98 psf), and the structure with interior partitions (91 psf), the ratio of experimental to calculated reduction factor is plotted in Fig. 3.4 for the three cases investigated. If the Engineering Method predicted the experimental results perfectly, this ratio would equal one for all detector positions. When this ratio is less than one, the calculational procedure is conservative, i.e., will predict dose rates higher than measured.

For the structure without interior partitions, the experimental reduction factors can be seen to be as much as 30 percent lower than the reduction factors calculated for detector positions near the 3 foot height above the floor. If the experimentally determined barrier factor were used in the calculations, the experimental reduction factors would be only 10 percent lower than the calculated reduction factors.

TABLE 3.1

INFINITE FIELD REDUCTION FACTORS - CONFIGURATION A

HEIGHT ABOVE FLOOR (FT.)	CASE 1	CASE 2	THEORY
FIRST FLOOR	EXP.	EXP.	CALC.
1	.051	.057	.055
2	.057	.067	.068
3	.060	.071	.074
4	.062	.075	.074
5	.063	.076	.072
6	.062	.075	.070
7	.062	.075	.067
8	.060	.072	.064
9	.059	.069	.059
SECOND FLOOR			
1	.028	.027	.036
2	.036	.040	.042
3	.040	.045	.046
4	.043	.049	.048
5	.045	.052	.050
6	.046	.054	.050
7	.047	.055	.049
8	.047	.056	.047
9	.046	.055	.045
10	.045	.051	.042
THIRD FLOOR			
1	.017	.015	.027
2	.025	.025	.032
3	.029	.032	.035
4	.032	.037	.038
5	.034	.040	.039
6	.036	.042	.039
7	.037	.044	.039
8	.038	.045	.038
9	.038	.045	.037
10	.036	.044	.034

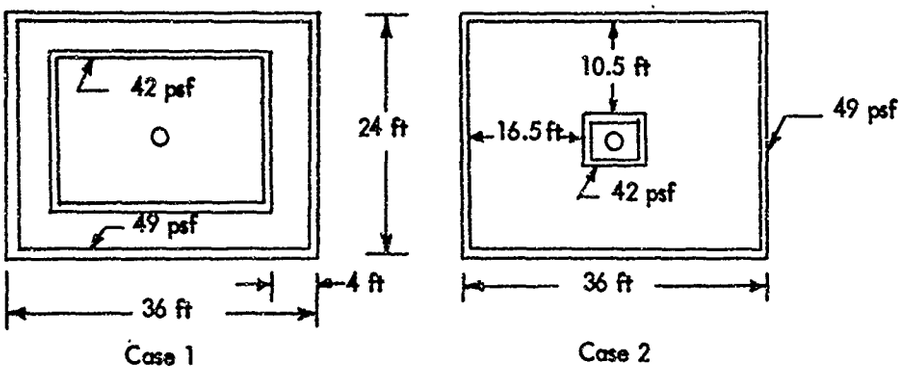

Configuration A

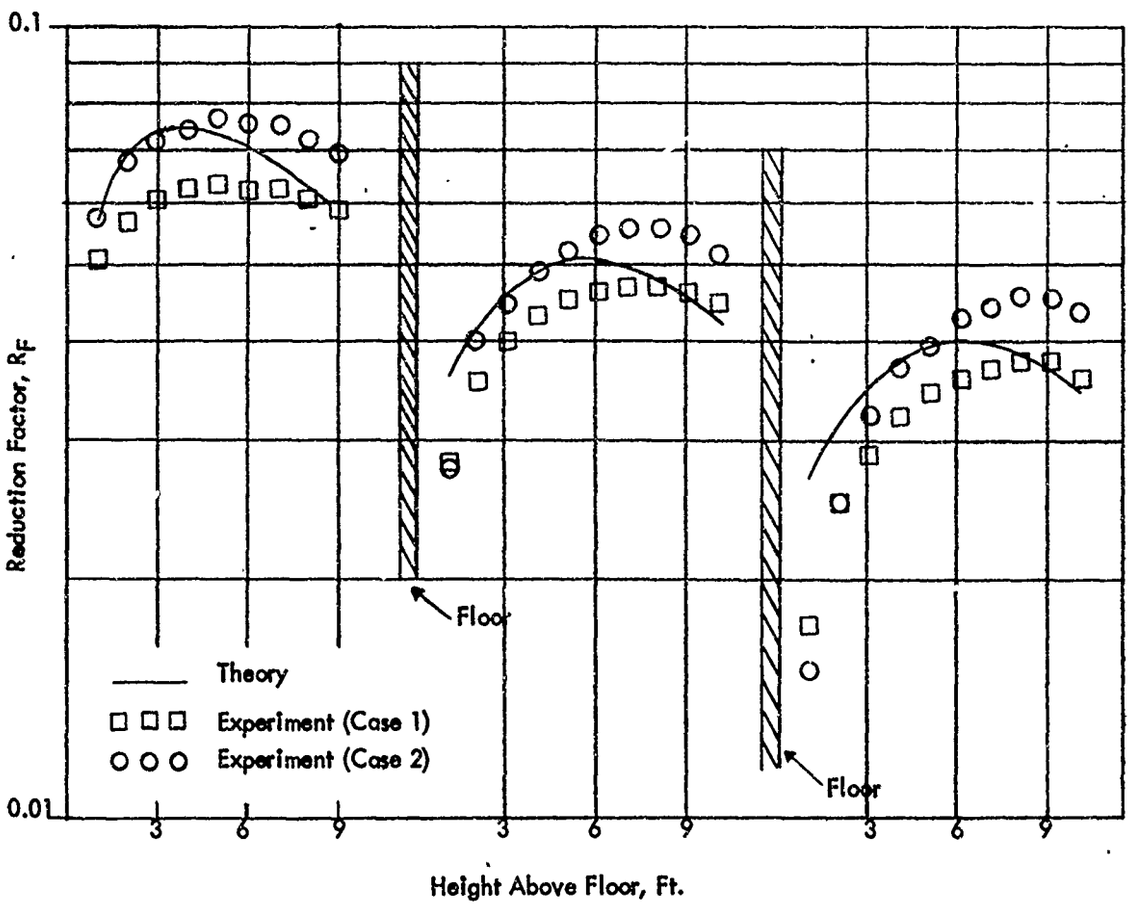

Figure 3.3 - Test Structure with Interior Partitions, 97.2 psf Floors

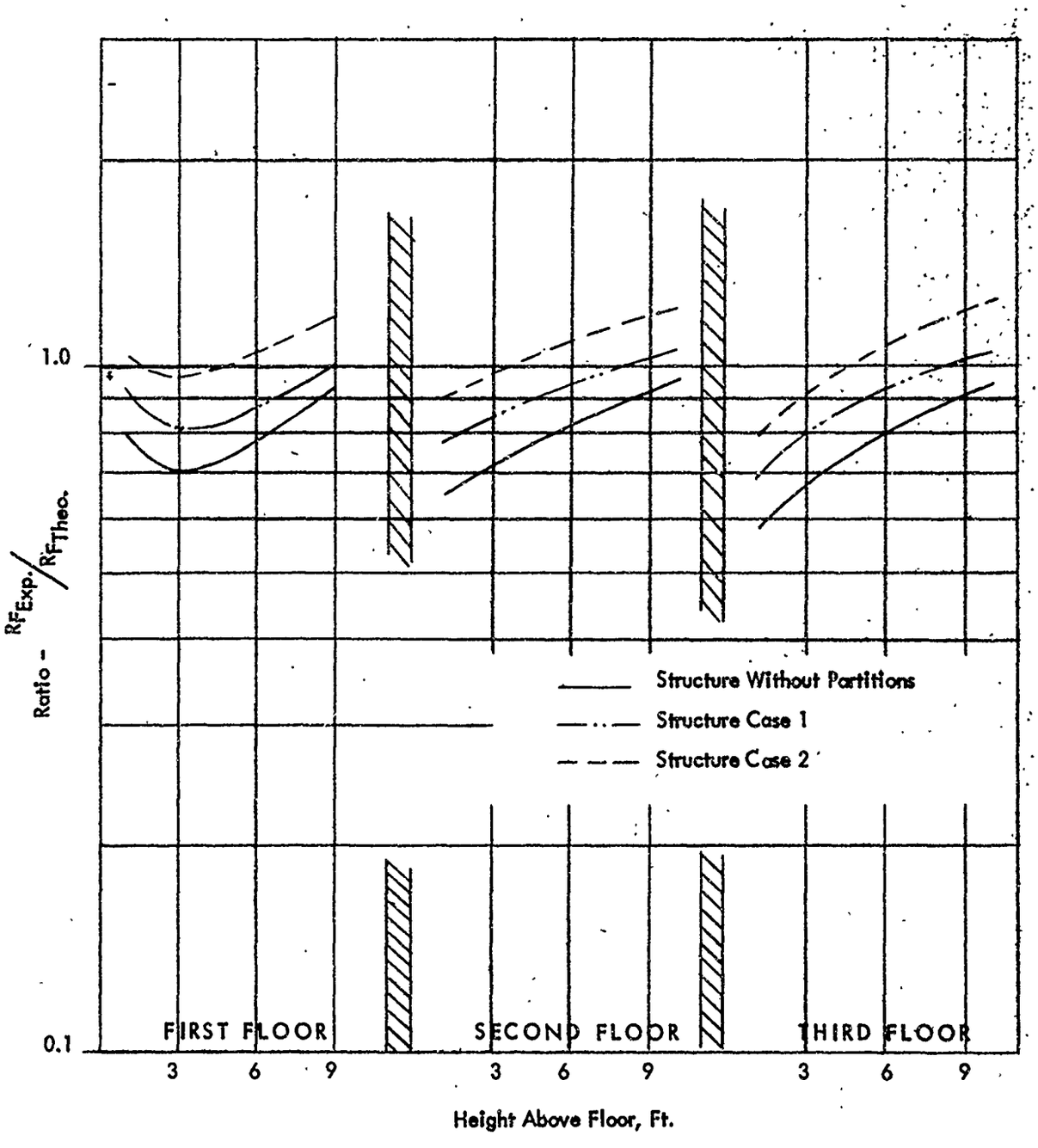

Figure 3.4 - Ratio of Experimental Reduction Factors to Theoretical Reduction Factors, Configuration A

For the structure with interior partitions, the ratio of experimental to calculated reduction factor approaches one as the partition is moved toward the detector. If a basic conservative error of 30 percent is assumed for the structure without interior partitions, the interior partition is increasing the dose rate to the detector and decreasing the conservatism in the method. Case 1 is of more practical interest than case 2 because of the size of the core area and, for this case, experimental values are 20 percent lower than theory. Thus, if the exterior wall barrier factor were corrected to agree closely with experiment[7], case 1 also would agree very well. Fig. 3.4 shows the same basic trends for upper floors as for the ground floors in the region of interest, i.e., 3 feet above the floor.

An experimental interior partition barrier factor was obtained from the results of the experiments on the structure with and without interior partitions. The ratio of reduction factors in the structure with interior partitions to that in the same structure without interior partitions is the interior partition barrier factor $B_i(X_j)$. These values are shown in Fig. 3.5 along with the calculated value $B_i(X_j,3')$. The experimental values in both cases do not vary with height above the ground except for positions near the floors, where local perturbations in dose rates caused by floor shadow can produce large experimental errors. These results verify the basic assumption that the interior partition barrier factor does not depend on detector height.

The effect of the interior partitions on the detector locations outside the central core area in case 1 was also investigated. Ratios of experimental reduction factors in the structure with interior partitions to those in the same structure without interior partitions are presented in Table 3.2 for three detector locations, as shown in the drawing accompanying Table 3.2. This ratio is less than one for all positions and stories of the structure, indicating that the interior partition effectively reduces the dose rate at these positions. The reduction in the corner of the structure (10, 15) amounts to approximately 20 percent whereas on the sides of the structure, (10, 0) and (0, 15), the attenuation afforded by the interior partitions reduced the dose rates by more than 30 percent. This reduction in dose rate effected by the partition is somewhat less on the second and third stories of the structure, where floor shadow and floor attenuation become factors.

Further analysis and comparisons with calculations for off-center detector locations will be reported at a later date.

Dose rates (expressed as reduction factors) recorded in the center of the test structure containing interior partition Configuration B (see Fig. 3.1b) are shown in Fig. 3.6 along with calculated values from Equation 3.5. The dose distribution as a function of the height above floors follow closely the results of experiments in Configuration A shown in Fig. 3.3. Again, as in Configuration A, Case 1, the agreement between calculated and experimental values at the 3-foot detector height is within 15 percent for all stories of the test structure.

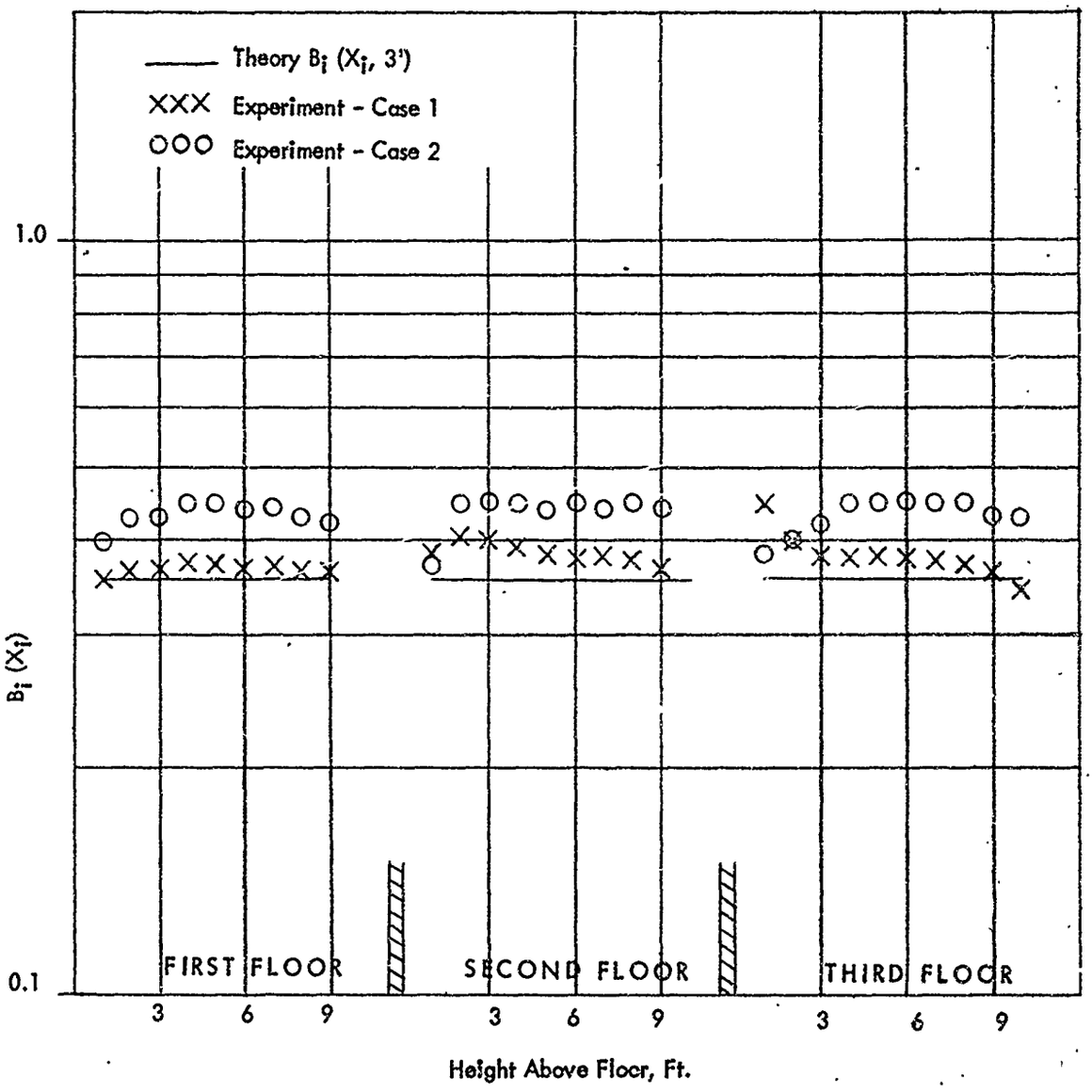

Figure 3.5 - Interior Partition Barrier Factor, Configuration A

TABLE 3.2

RATIO OF EXPERIMENTAL REDUCTION FACTORS
IN STRUCTURES WITH INTERIOR PARTITIONS TO THOSE IN STRUCTURES
WITHOUT INTERIOR PARTITIONS
CONFIGURATION A, CASE 1

HEIGHT ABOVE FLOOR (FT.)	DETECTOR POSITION		
	(10, 15)	(0, 15)	(10, 0)
FIRST FLOOR			
3	.794	.630	.645
6	.819	.672	.659
9	.810	.625	.718
SECOND FLOOR			
3	.900	.744	.824
6	.886	.784	.708
9	.864	.629	.678
THIRD FLOOR			
3	.929	.775	.743
6	.922	.765	.715
9	.840	.680	.677

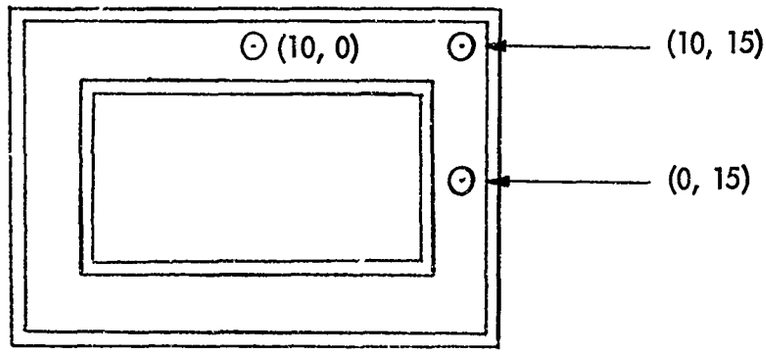

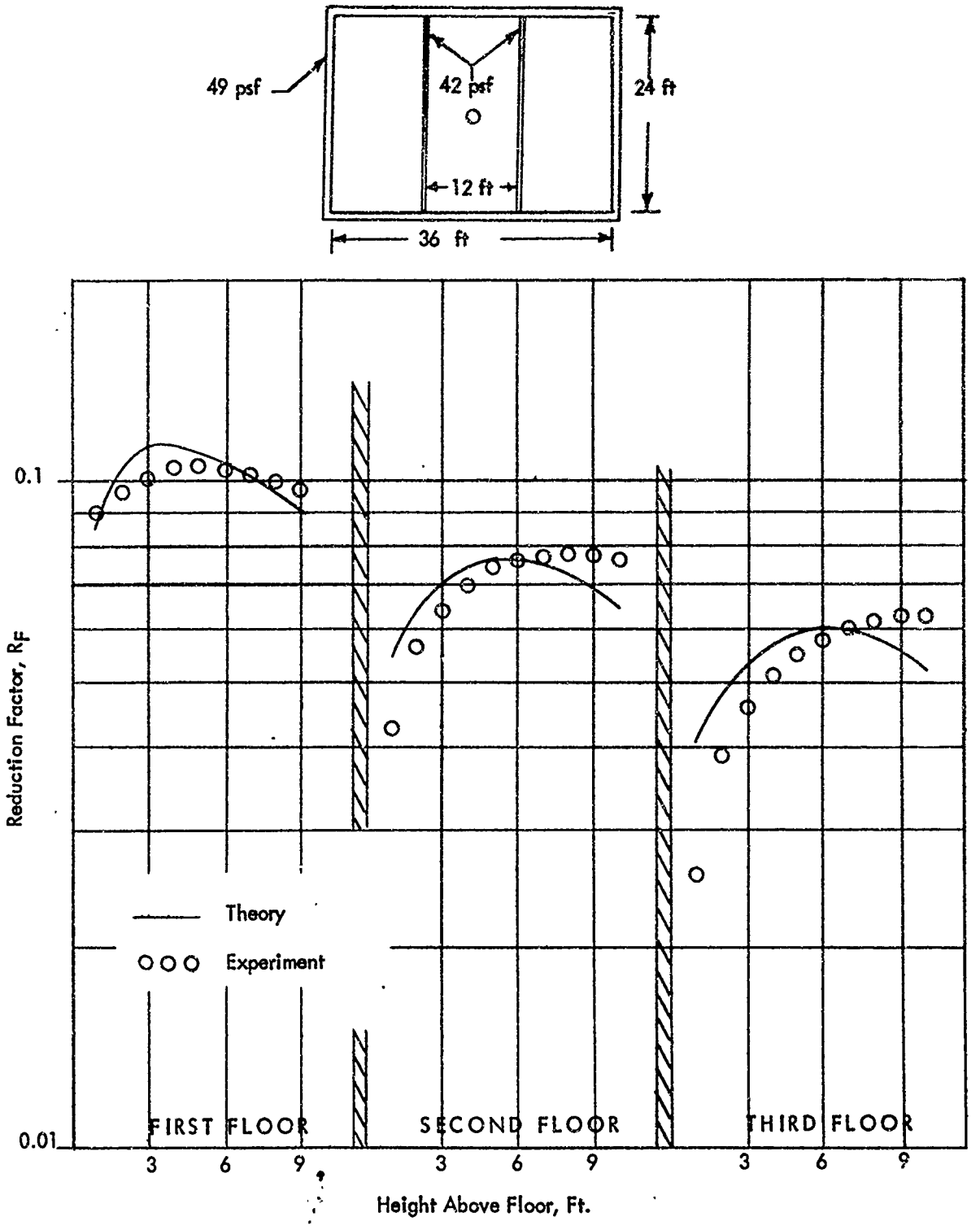

Figure 3.6 - Test Structure with Interior Partitions
Configuration B

Table 3.3 presents ratios of experimental reduction factors in the test structure with interior partition Configuration B to those in the same structure without interior partitions. These ratios are shown for three locations in the central room of the test structure. The results show that the placement of this partition configuration in the test structure reduced the dose rate in the center of the structure (0, 0) by 40 percent. Notice that the partitions in Configuration A, which completely surrounded the center detector, reduced the dose rate by more than 60 percent. These reductions in dose rates caused by interior partitions in the structure are in agreement with predicted reductions of 43 and 63 percent for Configuration B and A respectively.

Previous work[12] on the effect of interior partitions on the dose rate within a structure, agrees with the results of this study. This work was conducted by Technical Operations Research on a steel multistory structure, six stories high, each story being 1 foot high. Three interior partition configurations were evaluated: (1) a parallel partition arrangement similar to Configuration A of the RTF study; (2) a corridor partition arrangement similar to Configuration B of the RTF study; and (3) a compartmental partition arrangement. The exterior walls of the model structure were 20 psf thick and the floors were 80 psf thick. Interior partition mass thicknesses of 20, 40, and 60 psf were tested. In most cases, calculated results underestimated the experimental results by 8, 10, and 15 percent for the 20-, 40-, and 60-psf interior partition buildings, respectively. These differences are within the experimental error usually associated with model experiments.

The basic conclusion reached in analyzing the data of experiments conducted at the RTF is that the Engineering Method agrees with experiment for structures with interior partitions. The additional scattering provided by interior partitions that is not accounted for in the method is offset somewhat by the conservatism in values of the exterior wall barrier factor, $B_e(X_e)$. Thus, it seems that the inaccuracies introduced by the present simple method of treating interior partitions are not significant enough to warrant a change as long as both wall-scattered and direct radiation are used in their present form. This does not apply in below ground areas or for finite field radiation, where sizable errors may occur.

TABLE 3.3

RATIO OF EXPERIMENTAL REDUCTION FACTORS IN STRUCTURE WITH INTERIOR PARTITIONS TO THOSE IN SAME STRUCTURE WITHOUT PARTITIONS - CONFIGURATION B

HEIGHT ABOVE FLOOR (FT.)	DETECTOR POSITION		
	(0, 0)	(6, 0)	(10, 0)
FIRST FLOOR			
3	.613	.663	.766
6	.615	.684	.738
9	.611	.676	.750
SECOND FLOOR			
3	.645	.683	.800
6	.622	.702	.762
9	.605	.642	.741
THIRD FLOOR			
3	.621	.708	.788
6	.631	.678	.765
9	.609	.668	.752

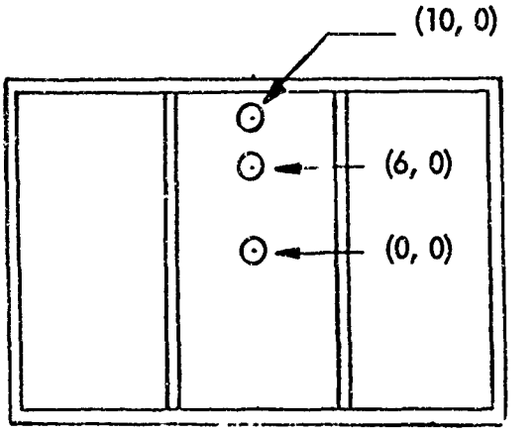

BLANK PAGE

CHAPTER 4

STRUCTURE WITH APERTURES

Apertures, in the form of windows and doorways, are present in all occupied structures. These apertures may decrease the protection given by the structure against ground based sources of radiation. The magnitude of the loss of protection and the locations within the structure in which it is noticed are of considerable importance in determining the shelter potential of the nonbasement portion of a building. Current structure shielding theory presents a method for calculating the effect of wall apertures on the radiation penetrating a structure. Experiments reported here were designed to evaluate the validity of this method.

4.1 THEORY

The detailed method for calculating the effects of wall apertures on the dose rate in a structure is presented in Reference 3. In brief, for a centrally located detector in a single story structure, the basic functional Equation 3.1 is used with a "differencing technique", which is applied to account for the apertures. The amount of radiation passing through and scattered by an aperture's area (as if it were solid) is subtracted from the contribution determined by Equation 3.1. To this figure, the unattenuated and unscattered radiation passing through the zero mass aperture area is added.

This technique involves the use of the additional solid angle fractions ω_a and ω_a' subtended at the detector by the top and bottom of the aperture. The drawing below illustrates the use of these and the other solid angle fractions.

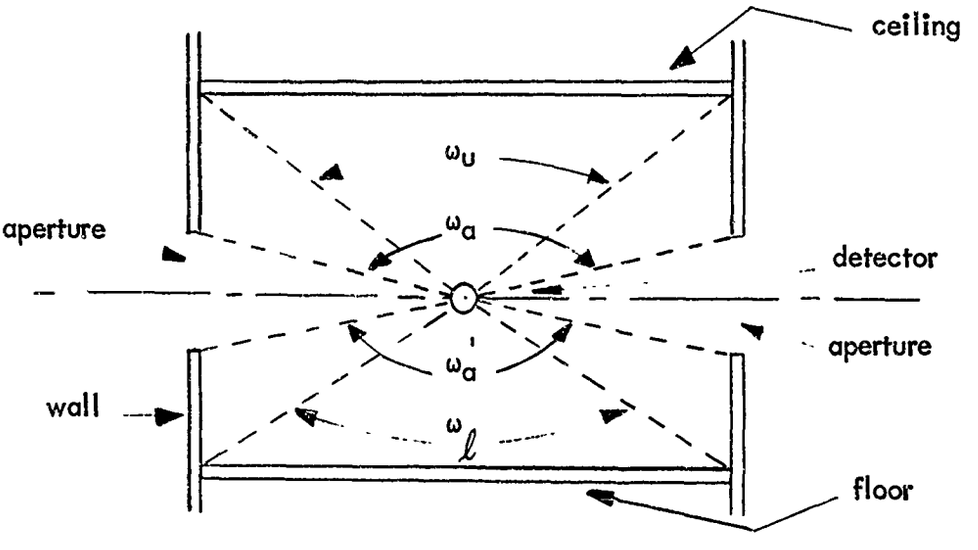

It is apparent that, in using this method, we assume that all the apertures are approximately uniformly spaced, have equal length, and are at the same height above the floor. A more complicated azimuthal sector analysis is recommended if these conditions are not present.

To account for the fact that most apertures have finite width, a perimeter ratio, P_a, is introduced. This is the ratio of the sum of the aperture widths to the building perimeter.

When the detector plane lies within the aperture (as shown in the sketch above), the differencing technique used to account for the apertures is applied as follows:

Let Equation 3.1 (the general functional equation) be represented by C_{g1}. Then the contribution from the "solid" aperture area is:

$$C_{g2} = B_e(X_e, H)\, P_a \left\{ \left[G_s(\omega_a) + (G_s(\omega_a') \right] \left[S_w(X_e) \right] \left[E(e) \right] + \left[G_a(\omega_a) + G_d(\omega_a', H) \right] \left[1 - S_w(X_e) \right] \right. \tag{4.1}$$

and the contribution from the "open" aperture area is:

$$C_{g3} = B_e(0, H)\, P_a \left[G_a(\omega_a) + G_d(\omega_a', H) \right] \tag{4.2}$$

The total reduction factor from ground based sources then is:

$$R_F = C_{g1} - C_{g2} + C_{g3} \tag{4.3}$$

The same method is used when the detector plane is above or below the aperture. The functional expressions for C_{g2} and C_{g3} will be altered to account for the absence of the contribution from direct or air scattered radiation.

In multistory structures with apertures on all floors, knowledge of the contributions from the floor above and the floor below the detector may be desired. This is usually a very small percentage of the dose rate, so a simpler, although less accurate, method is recommended. The "aperture percentage", A_p, is the ratio of aperture area to wall area on the floor in question. The contribution to the detector from the floor in question is calculated first as if the wall were all solid and second as if the wall were all aperture. The "all solid" portion is then multiplied by $(1 - A_p)$ and the "all aperture" portion by A_p. The sum of these terms therefore represents the contribution desired.

4.2 DESCRIPTION OF EXPERIMENT

The aperture experiments were performed on the full scale test structure described in Chapter 2 of this report. Fig. 4.1 shows the test structure with apertures in the exterior wall. These openings, on the first and second stories, are 4-foot squares placed with the sill at 4 feet above each floor and having 8 feet of solid wall between them. The perimeter ratio, P_a, is thus 1/3 and the aperture percentage, A_p, is 1/9. On the third story, the 4-foot-high aperture is again placed with the sill at about 4 feet above the floor level but here extends all around the building. On this floor, the perimeter ratio, P_a, is 1.0 and the aperture percentage, A_p, is 1/3.

Once again, the test structure in this experiment was comprised of 4-inch (49-psf) walls and 8-inch (97.2-psf) floors.

4.3 RESULTS AND ANALYSIS

The experimental results along the vertical centerline of the structure are shown in Table 4.1 and in Fig. 4.2, along with the calculated values. In general, the calculated results follow the trend of the experimental values and are about 15 percent (conservatively) high. The same general differences between theory and experiment have been noticed in previous studies (Reference 7) where apertures were not present. The "differencing" technique, therefore, appears to be a valid method for calculating the effect of apertures on the reduction factor in a structure.

Near each ceiling, the calculated values are relatively closer to the experimental values. This is probably caused by the assumption in the derivation of the Engineering Method that the wall scattered radiation, $G_s(\omega)$, is the same in the upward and downward directions. (see section 3.3).

An interesting ratio is shown in Fig. 4.3. This is the ratio of reduction factors on the centerline of the test structure with apertures to those in the same structure without apertures. Calculated as well as experimental results are shown. Below the sill height, as would be expected, this ratio, both theoretically and experimentally, is about 1.0 or slightly less. The presence of apertures would cause an increase in the contribution from skyshine and ceiling shine but a decrease in

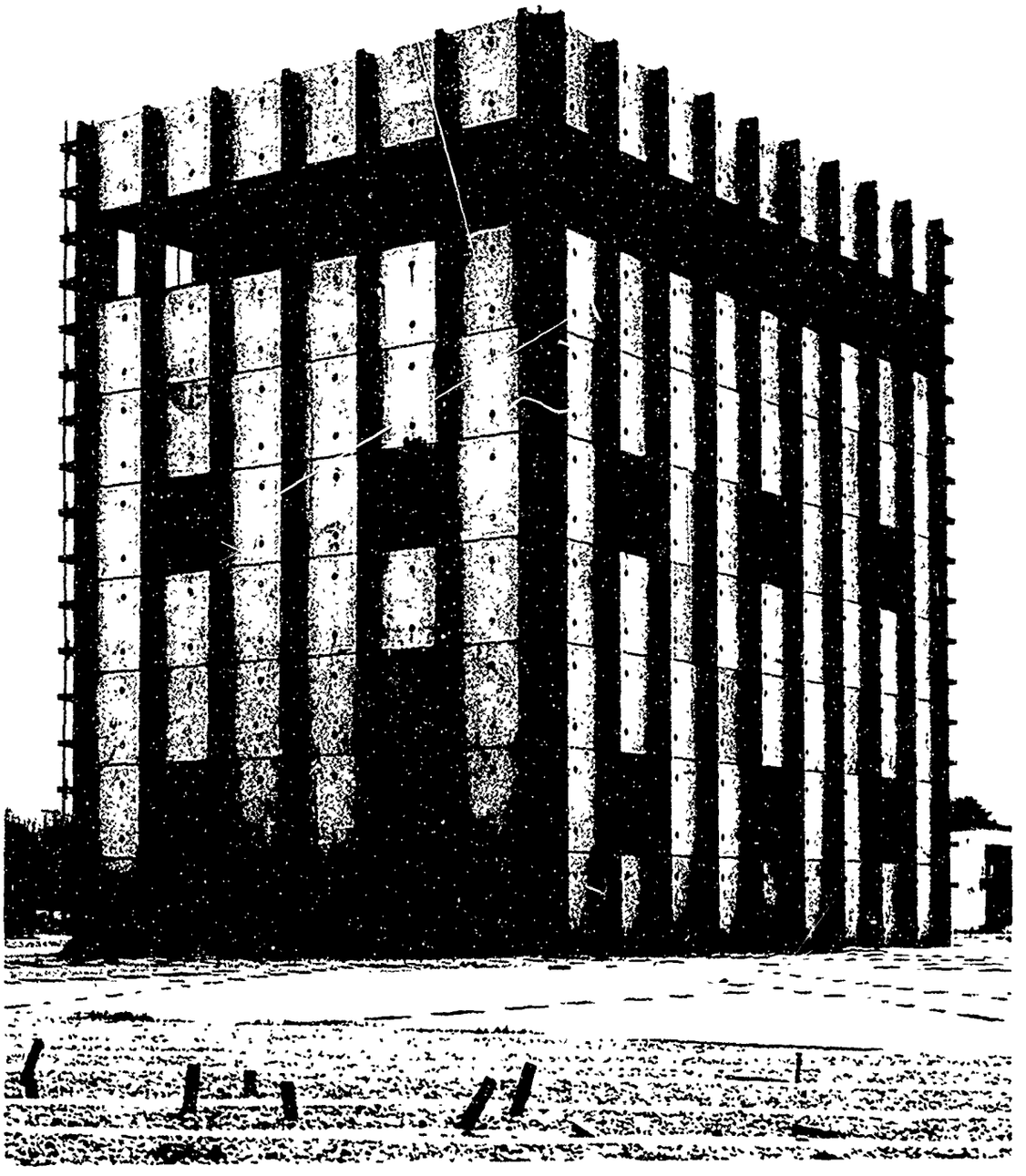

Figure 4.1 - Test Structure with Apertures

TABLE 4.1

INFINITE FIELD REDUCTION FACTORS
STRUCTURE WITH APERTURES

(CENTER DETECTOR POSITION)

STORY NUMBER	1		2		3	
Height Above Floor - ft.	EXP.	CALC.	EXP.	CALC.	EXP.	CALC.
1	.132	.153	.0677*	.0998	.0366	.0719
2	.149	.183	.0841*	.116	.0651	.0864
3	.155	.200	.0966	.127	.0767	.0949
4	.159	.197	.106	.135	.0866	.104
5	.208*	.275	.110	.154	.0932	.133
6	.230	.294	.153	.182	.143*	.191
7	.247	.298	.169	.199	.194	.236
8	.252	.293	.181	.207	.224	.272
9	.202	.241	.189	.199	.242	.277
10		.201	.168	.175	.239	.243

* Estimated from incomplete data

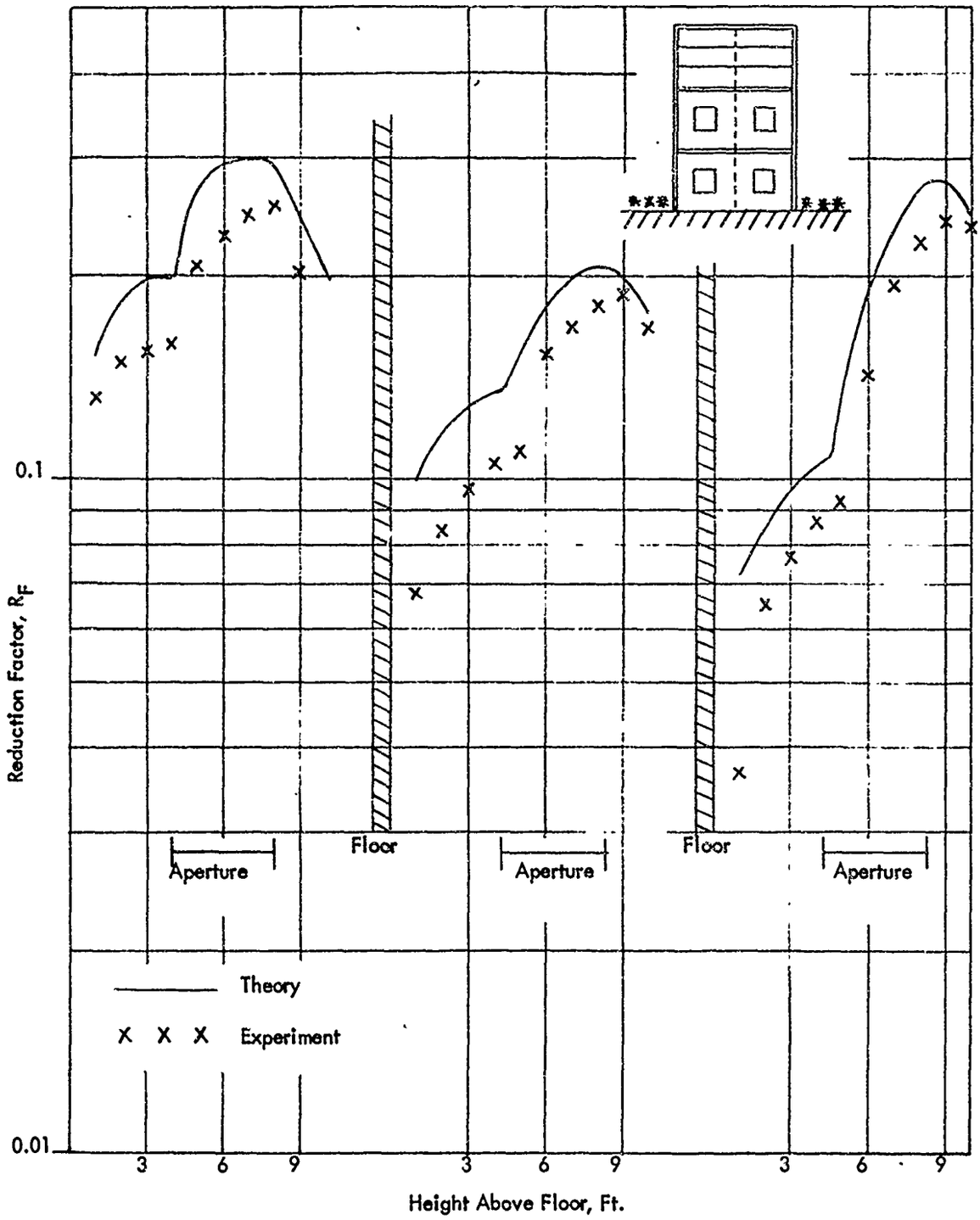

Figure 4.2 - Vertical Distribution of Reduction Factors on the Centerline of the Structure with Apertures

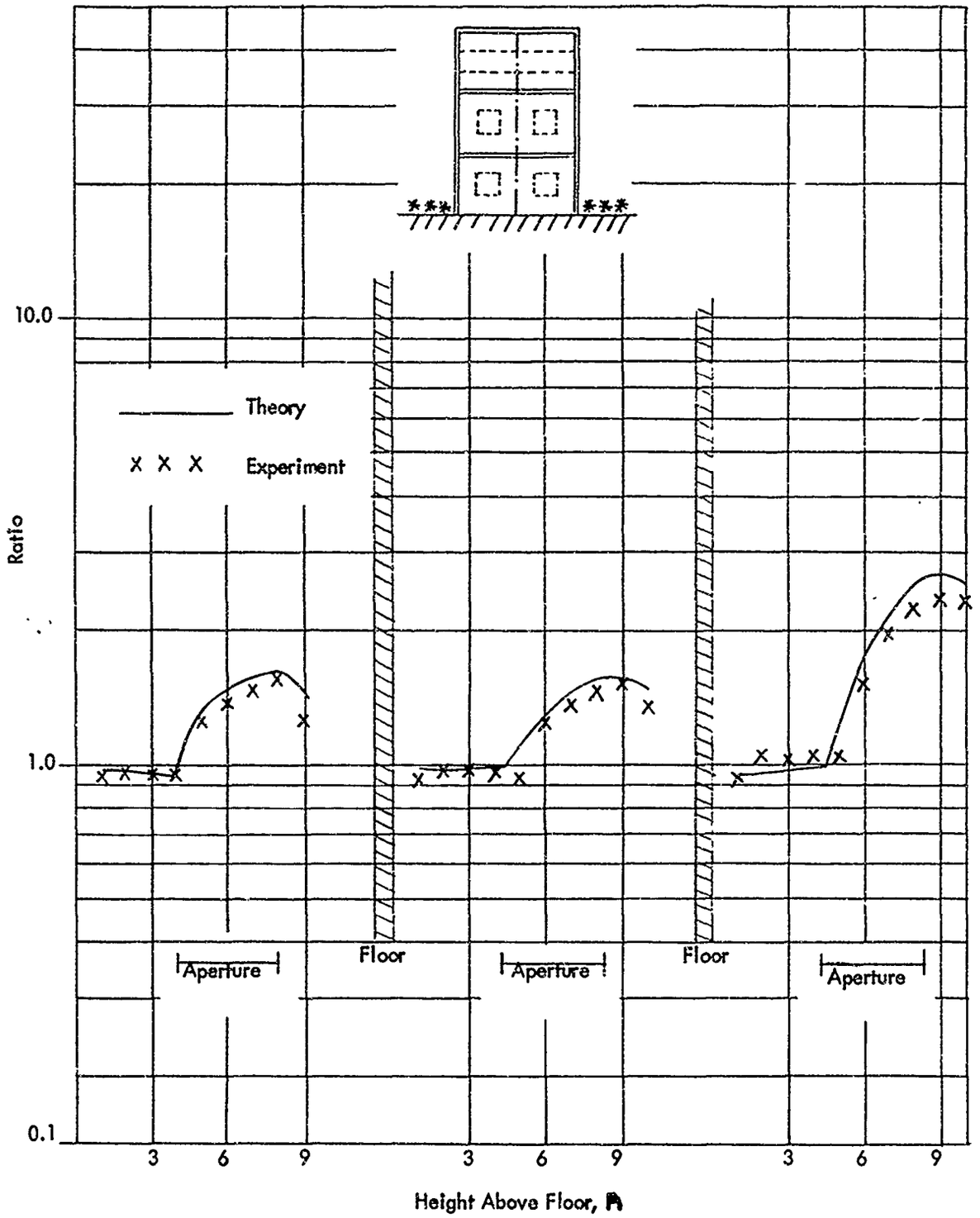

Figure 4.3 - Ratio of Reduction Factors in Structure with Apertures to Those in Same Structure Without Apertures

the wall scatter contribution. In this structure and with the aperture sizes investigated, these effects very nearly cancel each other.

When the detector is above the sill height, direct radiation passing through the aperture predominates and the above effects are negligible. On the first and second floors, where the windows take up 1/9 of the wall area, an increase of as much as 50 percent is found because of the added radiation. On the third floor, where the aperture fraction is 1/3, this ratio is as high as 2.35. The Engineering Method of calculation accounts quite well and conservatively for this effect. For the 1/9 aperture fraction, theory predicts as much as a 60-percent increase and, for the 1/3 aperture fraction, the ratio is 2.70.

In order to further investigate the effect of apertures on the reduction factor in a structure, the more realistic situation in which both apertures and interior partitions are present was investigated.

4.4 STRUCTURE WITH BOTH APERTURES AND INTERIOR PARTITIONS

Interior partitions were added to the test structure having apertures in the exterior wall. These interior partitions (Configuration A, Case 1) have been described in section 3.2. In short, they are 42 psf thick and are 4 feet from and parallel to the exterior wall. The exterior wall only has the apertures as described in section 4.2.

The Engineering Method handles the interior partitions in this case precisely as mentioned in section 3.1. The reduction factor without interior partitions is multiplied by $B_i(X_i)$. It is apparent, therefore, that the interior partition is treated solely as a barrier.

The experimental and calculated results are shown for the centerline of the structure in Table 4.2 and Fig. 4.4. As in the structure without interior partitions, the calculated values follow closely the trend of the experimental results but are less conservative. At a few locations, the calculations are actually nonconservative, although they do appear to lie within a range defined by the experimental error discussed in section 2.4, probably because scattering in the interior partition is not included in the calculation. This exclusion appears to be more significant to the calculation when part of the exterior wall is absent and direct radiation reaches the interior partition unscattered and unattenuated. Actually, much of this large quantity of relatively high energy radiation will scatter in the partition and travel to the detector. Particularly when the detector is below the sill height (and therefore is in the lower dose region), this contribution can be important.

This effect is more clearly visible in Fig. 4.5, which shows the ratio of the reduction factors in the structure with interior partitions and apertures to those in the same structure without apertures. Theoretically, according to the Engineering

TABLE 4.2

INFINITE FIELD REDUCTION FACTORS
STRUCTURE WITH APERTURES AND INTERIOR PARTITIONS

(CENTER DETECTOR POSITION)

STORY NUMBER	1		2		3	
Height Above Floor - Ft.	EXP.	CALC.	EXP.	CALC.	EXP.	CALC.
1	.0609	.0542	.0304	.0354	.0239	.0255
2	.0647	.0651	.0385	.0412	.0306	.0307
3	.068	.0711	.0423	.045	.0368	.0337
4	.0728	.070	.0456	.048	.0416	.0370
5	.0868	.0974	.0491	.0548	.0449	.0470
6	.0928	.104	.0629	.0646	.0538	.0679
7	.0977	.100	.0679	.0706	.0734	.0837
8	.0969	.104	.0697	.0733	.0872	.0966
9	.0832	.0856	.070	.0708	.0896	.0982
10		.0715	.0622	.062	.086	.0863

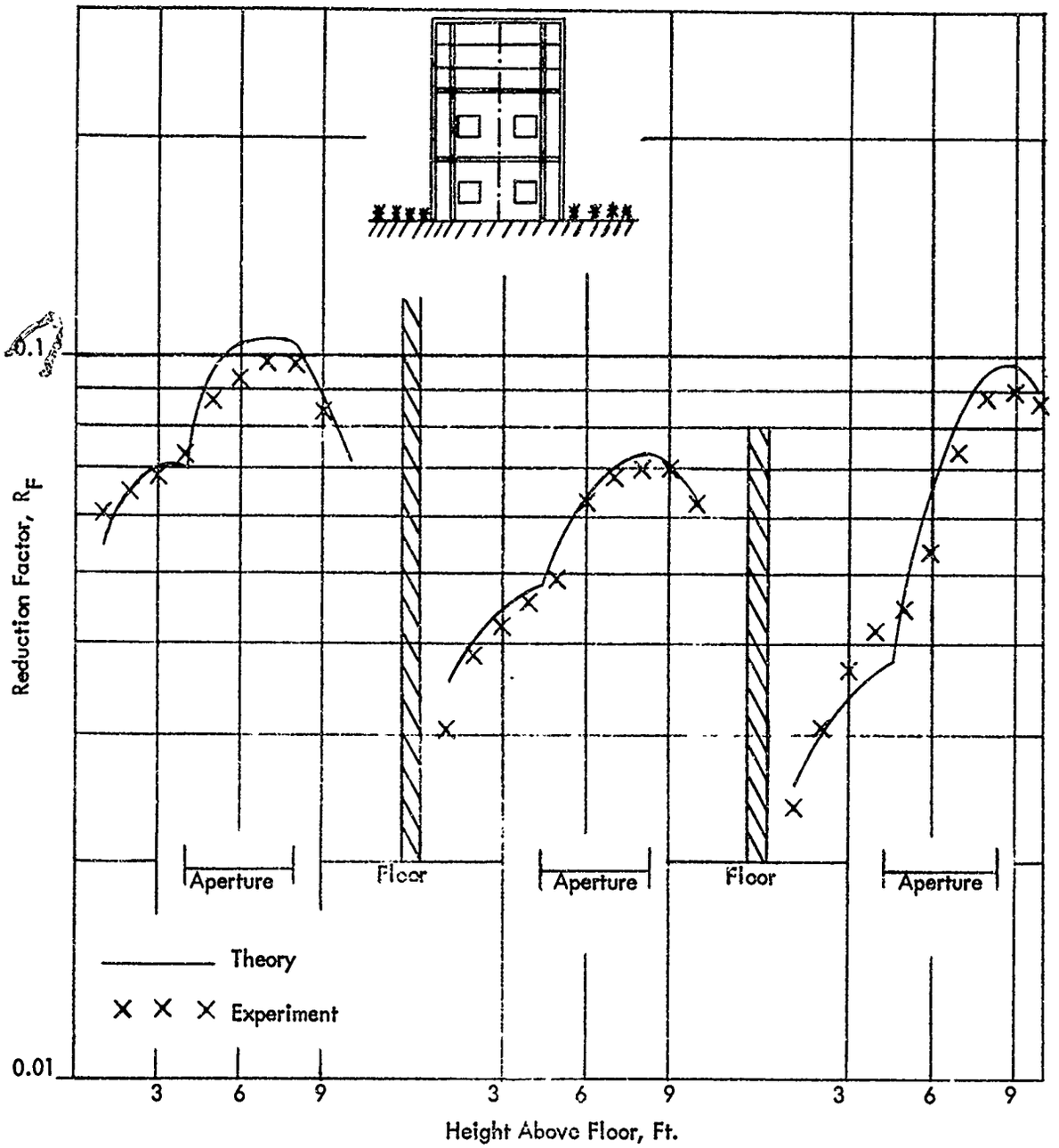

Figure 4.4 - Vertical Distribution of Reduction Factors
on the Centerline of the Structure
with Both Apertures and Interior Partitions

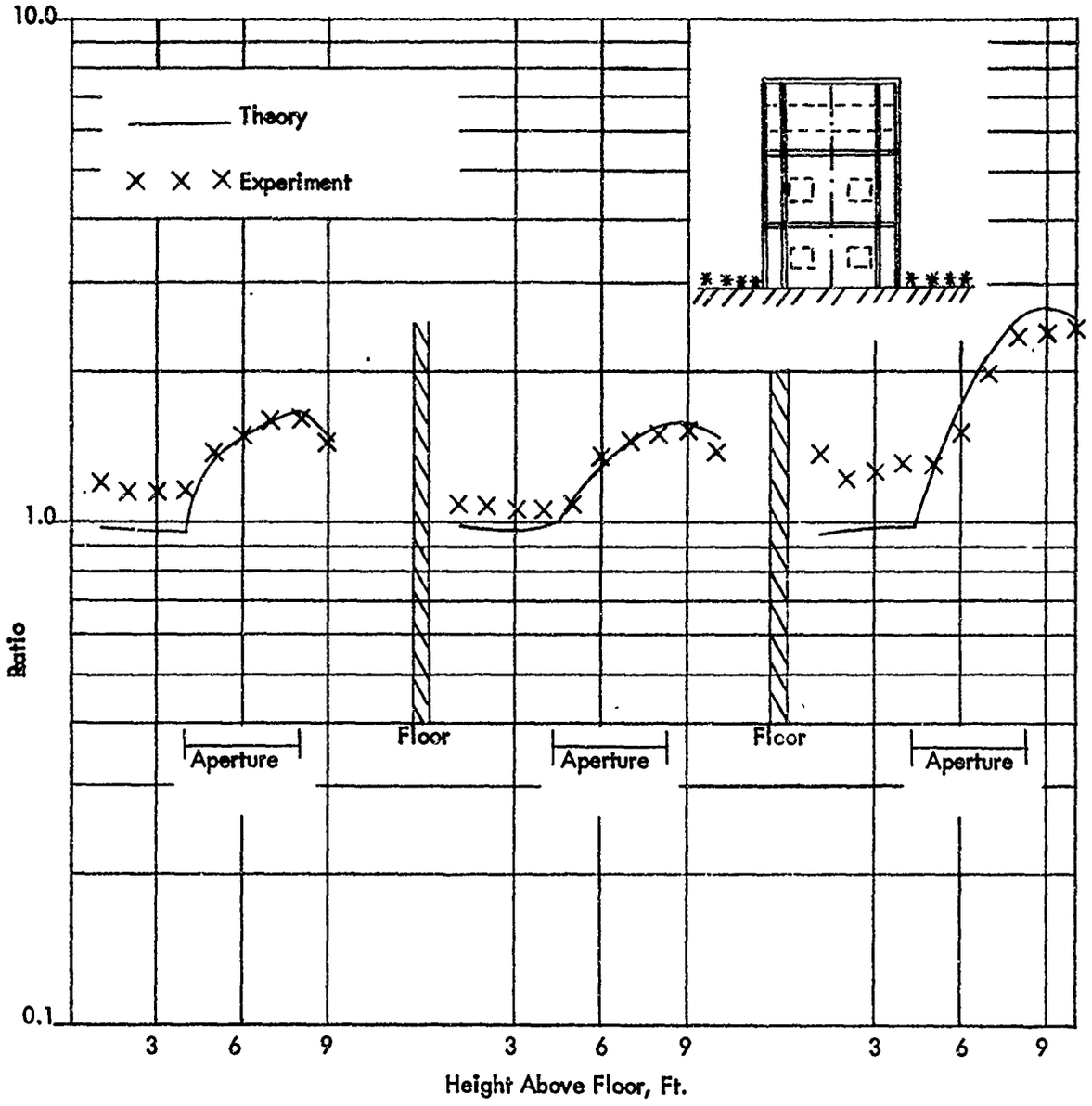

Figure 4.5 - Ratio of Reduction Factors in Structure with Interior Partitions and Apertures to those in Same Structure Without Apertures

Method of calculation, the ratio is identical to that shown in Fig. 4.3, where interior partitions are not present. Above the sill height of the aperture, this is experimentally shown to be true. The contribution from scattering in the interior partition in the window area is apparently small in relation to the greater effect of the direct radiation.

Below the sill height, where direct radiation through the aperture is not present, the component of the radiation scattered in the partition appears to have a greater effect. The calculated ratio underestimates the experimental by about 10 to 20 percent on the first and second floors (1/9 aperture percentage) and about 25 to 35 percent on the top floor (1/3 aperture percentage). It is highly probably that, were the structure to have a thicker exterior wall, particularly below the sill, these differences would become far greater. It is possible, therefore, that a location below the sill in a building may be calculated to be a shelter area whereas, in reality, it is not.

4.5 OFF-CENTER POSITIONS

As mentioned in section 2.3, measurements of the dose rate were made at various off-center locations (see Fig. 2.3) in the test structure. The reduction factors at these points are calculated by the "fictitious building" method described in Reference 3. Essentially, as shown in detail for the (6, 9) position in Appendix B of Reference 7, the building is divided into four imaginary structures symmetrical about the detector. The reduction factors for the imaginary buildings are calculated by the methods described in section 4.1 for the centerline. It is then assumed that the off-center reduction factor is the average of those calculated for the fictitious buildings. This "fictitious building" method has been found in the past (Reference 7) to be valid in predicting reduction factors at off-center positions from ground based sources of radiation.

The measured dose rates at all the off-center positions in the structure are tabulated in Appendix A. Table 4.3 and Figs. 4.6 and 4.7 show a comparison of the experimental and calculated reduction factors at two of these positions (10, 0) and (6, 9). Position (10, 0) is outside the partitioned area (when present) and position (6, 9) is within it. The (10, 0) position is directly in front of an aperture.

Again, as with the center of the structure discussed in sections 4.3 and 4.4, the calculations are somewhat conservative, especially when the interior partition is not present. From this series of experiments, we conclude that the "fictitious building" method is valid for predicting off-center reduction factors in a structure with apertures.

TABLE 4.3

INFINITE FIELD REDUCTION FACTORS - OFF CENTER POSITIONS —
STRUCTURE WITH APERTURES
WITH AND WITHOUT INTERIOR PARTITIONS

Height Above Floor-Ft.	POSITION (10, 0)				POSITION (6, 9)			
	Without Interior Partitions		With Interior Partitions		Without Interior Partitions		With Interior Partitions	
	EXP.	CALC.	EXP.	CALC.	EXP.	CALC.	EXP.	CALC.
1	.122	.179	.104	.129				
2	.144	.204	.115	.144				
3	.154	.229	.124	.162	.148	.216	.0674	.0767
4	.158	.218	.126	.151				
5	.261	.362	.207	.271				
6	.283*	.383	.219	.286	.233	.320	.0995	.114
7	.290	.396	.222	.290				
8	.261	.384	.200	.284				
9	.195	.265	.133	.181	.196	.255	.0864*	.0905
10	.176*	.213	.116	.141				
1	.0703*	.114	.0716	.0811				
2	.0882	.134	.0875	.0963				
3	.107	.142	.0901	.101	.105	.138	.0474	.0491
4	.121*+	.149+	.0919+	.105+				
5	.171 +	.223+	.156+	.172+				
6	.199 +	.258+	.180+	.199+	.156	.201	.0661	.0714
7	.213 +	.275+	.185*+	.210+				
8	.212 +	.282+	.181+	.213+				
9	.167 +	.215+	.123+	.151+	.159	.215	.0691*	.0763
10	.156 +	.172+	.121+	.113+				
3	.0883	.111	.0691	.0798	.0859	.110	.0363	.0391
4	.0987*+	.119+	.0777+	.0852+				
6	.189	.266	.167	.213	.165	.244	.0674	.0866
9	.218	.303	.156	.215	.241*	.304	.0853*	.108

* Estimated From Incomplete Data
\+ Detector is Four Inches Higher than Stated

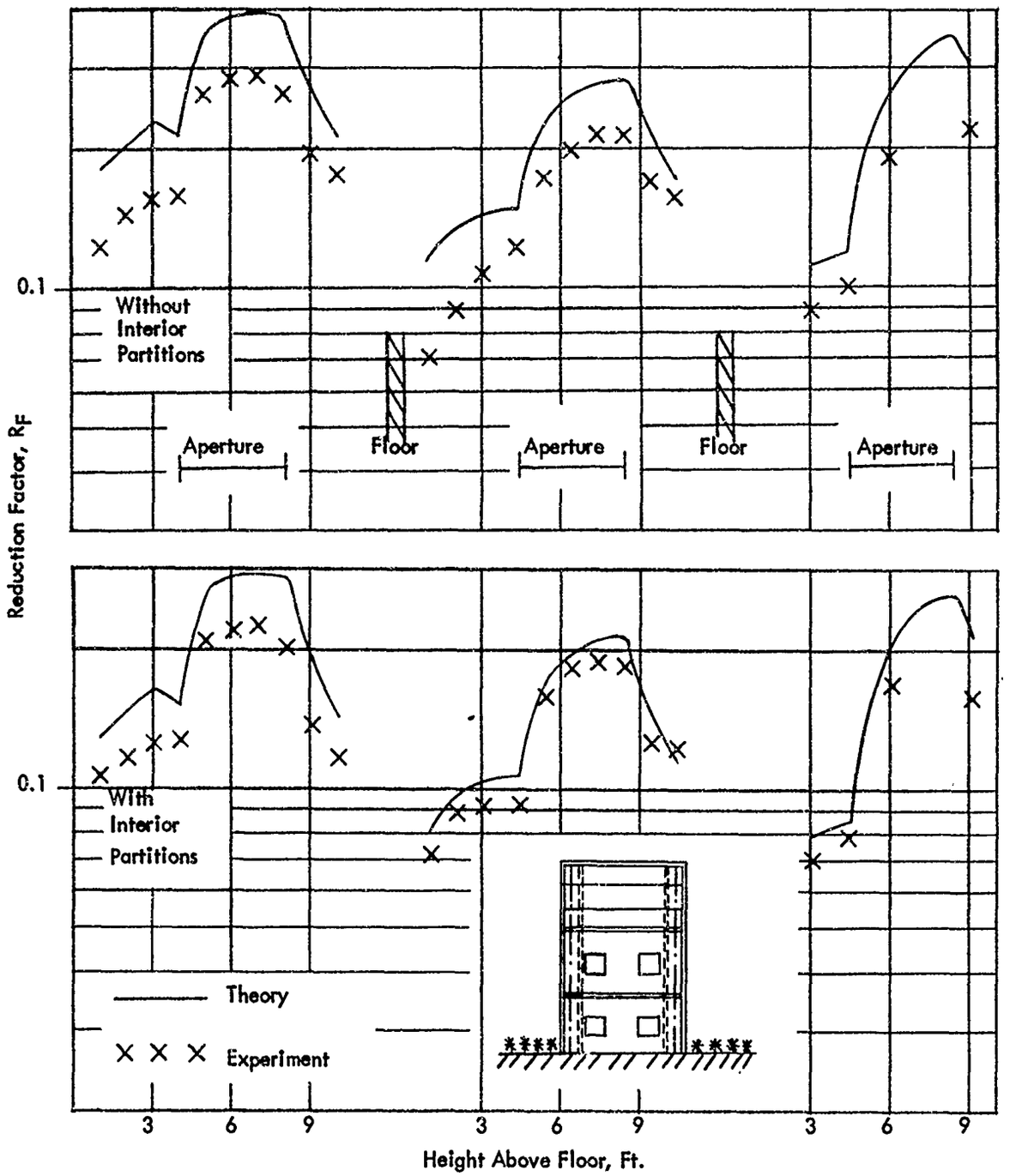

Figure 4.6 - Vertical Distribution of Reduction Factors at the (10, 0) Position of the Structure with Apertures with and Without Interior Partitions

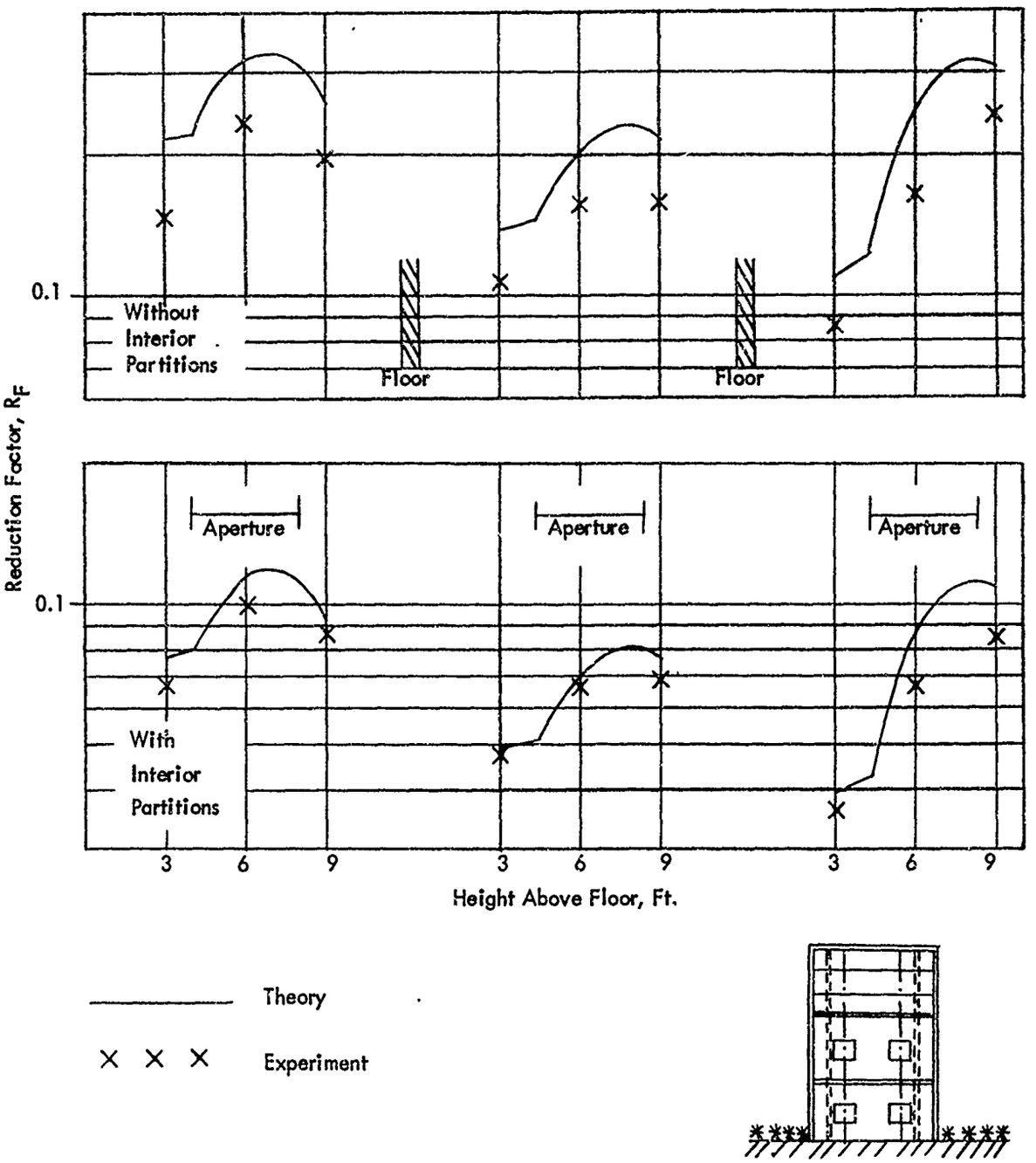

Figure 4.7 - Vertical Distribution of Reduction Factors at the (6, 9) Position of the Structure with Apertures with and Without Interior Partitions

4.6 COMPARISON WITH PREVIOUS WORK

An experimental investigation of the effects of apertures on reduction factors in structures with and without interior partitions was made by Technical Operations Research[11]. This work was conducted with a steel model cylinder 2 feet in diameter and 2 feet high. A 2-foot-diameter steel cylinder, of the same height as the larger and concentric with it, was employed as an interior partition. The exterior wall thicknesses used were 20, 40, and 60 psf. The interior partition, when present, was 20 psf thick. The infinite plane of radiation was simulated by cobalt-60 point sources out to a radius of 50 feet. Corrections were then applied to extrapolate the source plane to infinity. These experiments used 6-inch-high apertures extending around the entire outer wall at locations 0-6, 6-12, 12-18, and 18-24 inches above the ground.

When the interior partition was not present, the calculations predicted well the trend and magnitude of the experimental results. These calculations, however, were less conservative than those shown for the RTF full-scale structure in Fig. 4.2. When the interior partition was in place, the calculations, although following the trend of the experimental results, underestimated the experimental reduction factors by as much as a factor of two.

Since the models utilized had no roof, skyshine could raise the experimental values more than predicted by the Engineering Method of calculation. In addition, later study of the far-field correction has shown that the experimental reduction factors should be lower than those reported.*

At any rate, the general characteristics of the results of the model work are similar to those discussed here for full-scale structures. The presence of an interior partition reduces the dose rate in a structure with apertures by less than the calculations would predict. The discrepancy appears to be greater in the model work but, again, this observation may be misleading.

---

* Personal communication, A. L. Kaplan, Technical Operations Research, Burlington, Massachusetts (July 17, 1968)

CHAPTER 5

STRUCTURE WITH NONUNIFORM WALLS

Many structures have nonuniformities in wall thickness for a variety of reasons. If these are much thinner or thicker than the uniform thickness of the wall or if they cover a relatively large area of the wall, they must be considered in calculating reduction factors for the building. A series of experiments have been run on the full-scale structure at the RTF to evaluate the sector analysis method, proposed by current structure shielding theory, for handling nonuniform walls.

5.1 THEORY

The sector analysis method of calculating the reduction factor in a structure with nonuniform walls is presented in Reference 3. Essentially, the structure is investigated as a group of fictitious buildings each with a uniform wall thickness equivalent to one of the thicknesses in the original structure. The reduction factor for each of these imaginary structures is calculated by the standard method (Equation 3.1 for a simple structure). A weighted average reduction factor is then obtained by considering the azimuthal sector, derived from a 360° scan of the walls about the detector, of each thickness involved. The azimuth encompassing a particular thickness is divided by 360° to give the fraction of that fictitious building contributing to the total reduction factor.

For a structure with two mass thicknesses in the wall, consider this simple structure:

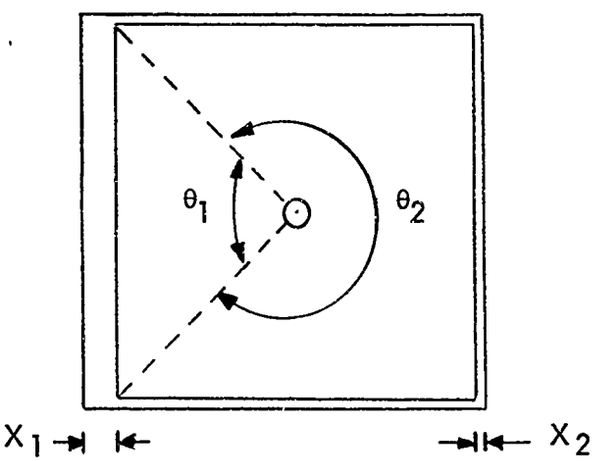

One wall has mass thickness, X_1, and the other three have thickness, X_2. A 360° scan about the detector yields an azimuth, θ_1, equal to 90° for the thicker wall and consequently $\theta_2 = 270°$ for the remaining. The azimuthal sectors are therefore:

$$A_{Z1} = \frac{\theta_1}{360°} = \frac{90°}{360°} = 0.25 \qquad (5.1)$$

and

$$A_{Z2} = \frac{\theta_2}{360°} = \frac{270°}{360°} = 0.75 \qquad (5.2)$$

The fictitious buildings, each of wall thickness, X_1 and X_2, would have reduction factors of C_{g1} and C_{g2} respectively. The total weighted average reduction factor would then be:

$$R_F = A_{Z1} C_{g1} + A_{Z2} C_{g2} \qquad (5.3)$$

5.2 DESCRIPTION OF EXPERIMENT

The nonuniform wall experiments were performed on the full-scale test structure described in Chapter 2 of this report. The 4-inch wall structure was altered by the addition of 4-foot-wide concrete slabs, 4 inches thick, centered in each 12 feet of wall span. The resulting nonuniform wall structure, a plan view of which is shown in Fig. 5.1, had 1/3 of its wall 8 inches (98 psf) thick and 2/3 was 4 inches (49 psf) in thickness.

The sum of the azimuthal sectors (also shown in Fig. 5.1) of the 4 inch section is 0.67 and, of the 8-inch section, 0.33.

5.3 RESULTS AND ANALYSIS

The experimental results along the centerline of the structure are shown in Table 5.1 and Fig. 5.2 along with the values calculated by the azimuthal sector technique. The theoretical agreement with experiment is about the same as that noticed in previous experiments.[7] The calculations are about 30 percent conservative except at positions near each ceiling, where the assumptions inherent in the $G_s(\omega)$ expression tend to lower the reduction factor. This effect has been discussed in sections 3.3 and 4.3 of this report. The agreement between the experimental results and the calculated values indicates that the method of azimuthal sectors is valid for predicting the dose rates along the centerline of a structure having nonuniform exterior walls in the thickness ranges utilized here.

TABLE 5.1

INFINITE FIELD REDUCTION FACTORS
STRUCTURE WITH NONUNIFORM WALLS

(CENTER DETECTOR POSITIONS)

STORY NUMBER	1		2		3	
Height Above Floor - Ft.	EXP.	CALC.	EXP.	CALC.	EXP.	CALC.
1	.104	.119	.0511	.0777	.0309	.0583
2	.112	.145	.0662	.0910	.0479	.0683
3	.119	.159	.0782	.0986	.0583	.0758
4	.123	.158	.0854	.104	.0639	.0808
5	.124	.154	.0885	.107	.0691	.0843
6	.121	.149	.0916	.106	.0743	.0846
7	.121	.143	.0948	.105	.0779	.0844
8	.120	.135	.0956	.101	.0784	.0819
9	.117	.125	.0954	.0960	.0800	.0782
10			.0940	.0893	.0811	.0729

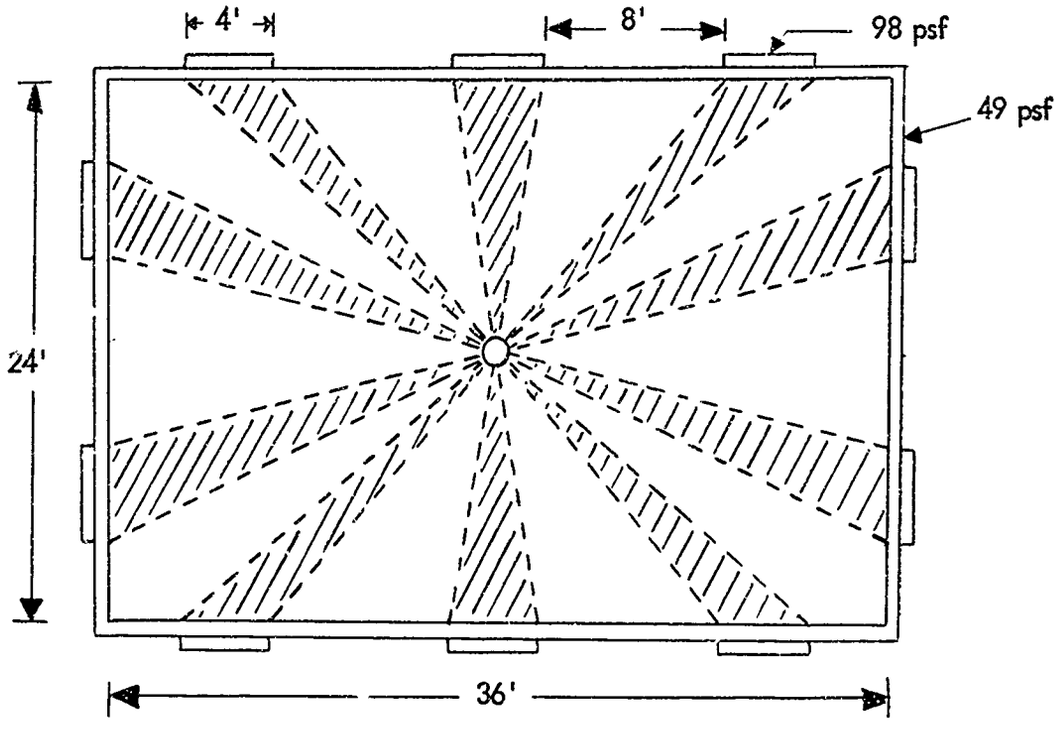

Figure 5.1 - Plan View - Structure with Nonuniform Walls

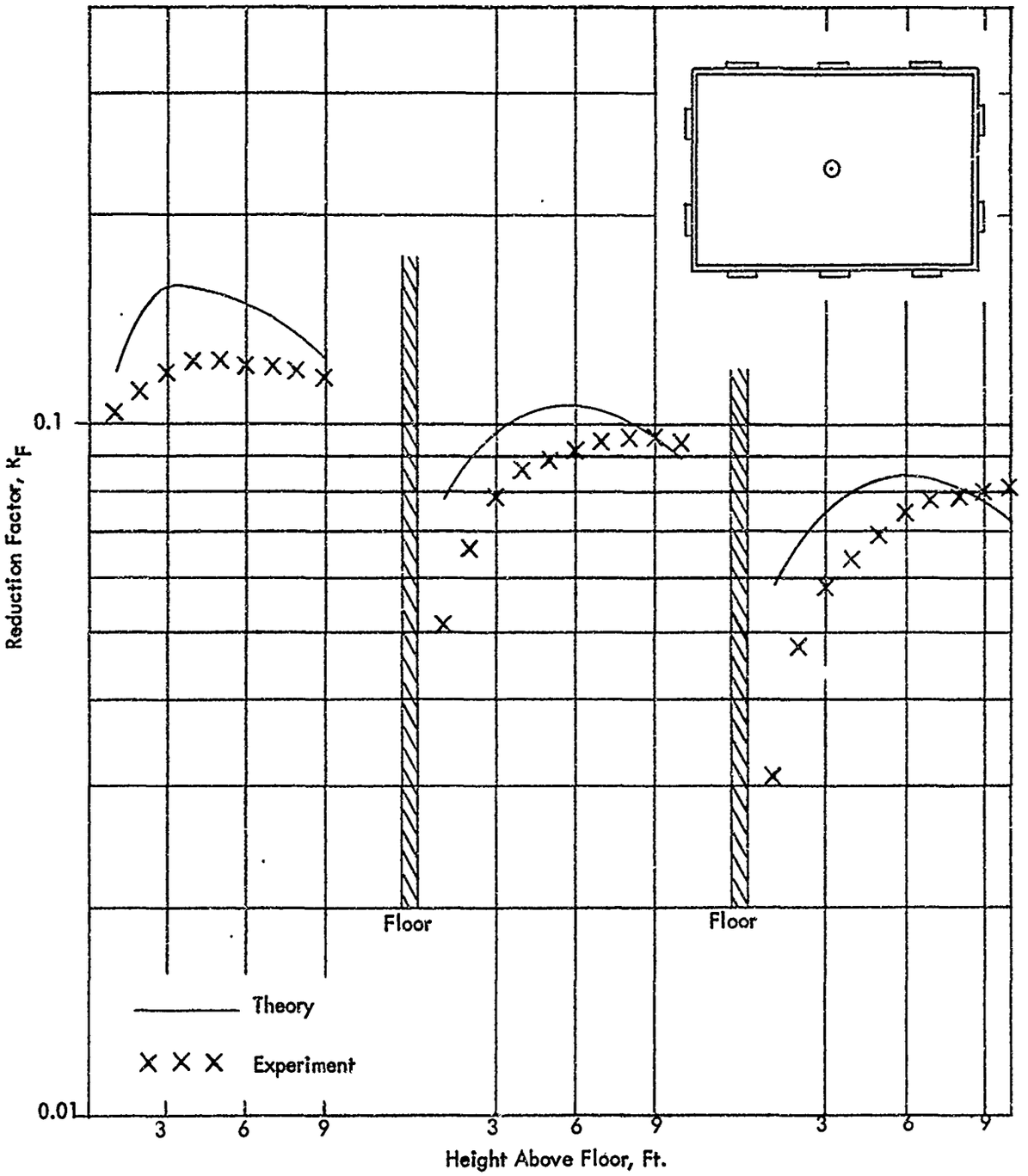

Figure 5.2 - Vertical Distribution of Reduction Factors on the Centerline of the Structure with Nonuniform Walls

5.4 STRUCTURE WITH NONUNIFORM WALLS AND INTERIOR PARTITIONS

The test structure as described above was modified by adding a 42-psf interior partition. As described in section 3.2, this partition (Configuration A, Case 1) was placed 4 feet from the exterior wall and parallel to it.

The Engineering Method of calculation handles this situation as discussed in section 3.1. The reduction factor for the structure without interior partitions is multiplied by $B_i(X_i)$.

The results of the experiment for the structure centerline are shown in Table 5.2 and Fig. 5.3 along with the calculated values. For this case, theory is about 20 percent conservative at locations other than near the ceilings. The agreement closer than that observed in Fig. 5.2, probably results from the assumption in the Engineering Method that the interior partition be treated only as an absorber. For the nonuniform wall configuration, this assumption is evidently not so extreme, as to yield highly inaccurate results.

The ratio of the reduction factors in the structure with interior partitions to the reduction factors in the same structure without the partition is the interior partition barrier factor, $B_i(X_i)$. The experimental barrier factor has been discussed in Chapter 3 for an exterior wall of uniform thickness. The ratio shown in Fig. 5.4 for a nonuniform wall is essentially the same as for the uniform 4-inch outer wall. It is noteworthy that (in agreement with theory) these variations in the outer wall do not appreciably change the magnitude or shape of the interior partition barrier factor on the centerline of the structure.

5.5 OFF-CENTER POSITIONS

Dose rates were measured both at the centerline and at various off-center locations in the structure (see section 2.3). Again, the reduction factors for these positions were calculated by the "fictitious building" method described in References 3 and 7.

The dose rates measured at all the off-center locations are tabulated in Appendix A. For positions (6, 9) and (10, 15), the experimental and calculated reduction factors are shown in Table 5.3 and Figs. 5.5 and 5.6. In general, the agreement between the Engineering Method and experiment, with and without interior partitions, is about the same as that noticed for the centerline of the structure. One may therefore surmise that the "fictitious building" method is valid for calculating the reduction factors at off-center locations in structures with nonuniform outer walls, as well as for those with uniform walls[7].

TABLE 5.2

INFINITE FIELD REDUCTION FACTORS
STRUCTURE WITH NONUNIFORM WALLS AND INTERIOR PARTITIONS

(CENTER DETECTOR POSITION)

STORY NUMBER	1		2		3	
Height Above Floor - Ft.	EXP.	CALC.	EXP.	CALC.	EXP.	CALC.
1	.0407	.0422	.0212	.0276	.0141	.0207
2	.0438	.0515	.0270	.0323	.0194	.0242
3	.0460	.0564	.0298	.0350	.0228	.0269
4	.0477	.0561	.0321	.0369	.0250	.0286
5	.0481	.0546	.0335	.0380	.0264	.0299
6	.0471	.0529	.0347	.0376	.0276	.0300
7	.0470	.0507	.0352	.0372	.0284	.0299
8	.0457	.0479	.0351	.0358	.0287	.0290
9	.0432	.0443	.0347	.0340	.0283	.0278
10			.0332	.0316	.0274	.0258

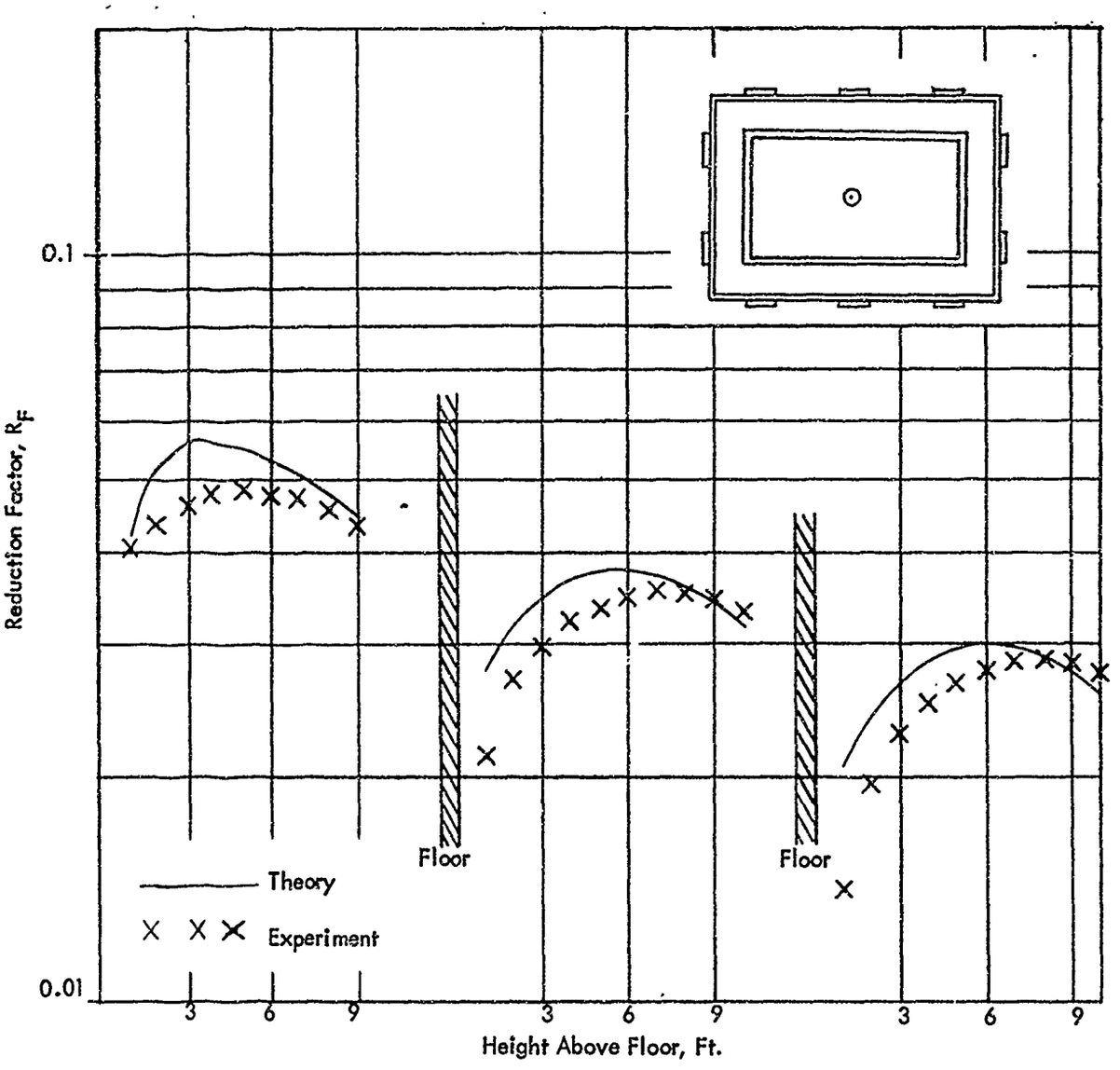

Figure 5.3 - Vertical Distribution of Reduction Factors
on the Centerline of the Structure
with both Nonuniform Walls and Interior Partitions

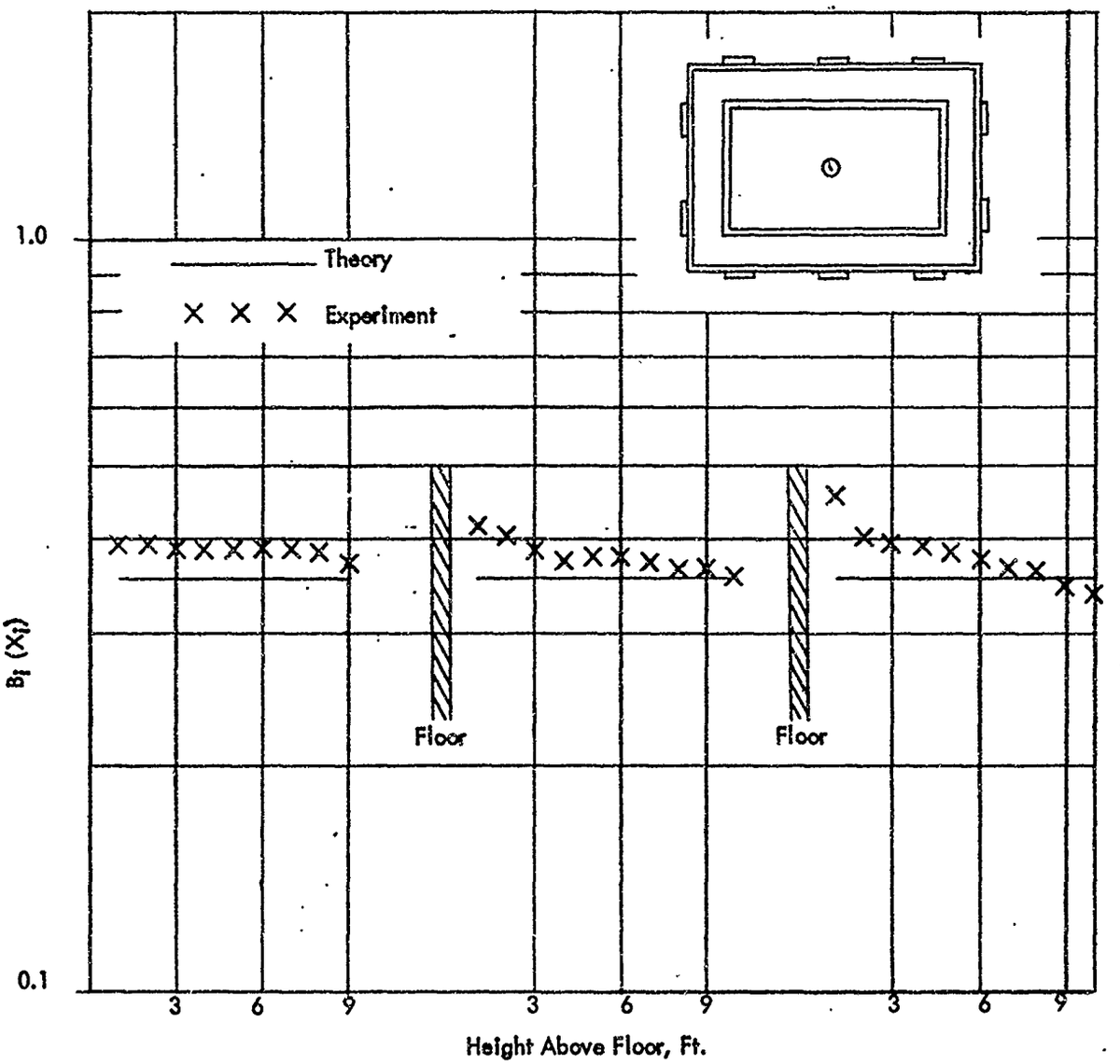

Figure 5.4 – Experimental Interior Partition Barrier Factor — Structure with Nonuniform Exterior Walls

TABLE 5.3

INFINITE FIELD REDUCTION FACTORS - OFF CENTER POSITIONS —
STRUCTURE WITH NONUNIFORM WALLS
WITH AND WITHOUT INTERIOR PARTITIONS

Height Above Floor - FT.	POSITION (6, 9)				POSITION (10, 15)			
	Without Interior Partitions		With Interior Partitions		Without Interior Partitions		With Interior Partitions	
	EXP.	CALC.	EXP.	CALC.	EXP.	CALC.	EXP.	CALC.
3	.119	.168	.043*	.060	.144	.204	.130	.182
6	.129	.157	.047*	.056	.145	.184	.128	.164
9	.121	.131	.044*	.046	.134	.156	.118	.138
3	.0835	.105	.032	.037	.104	.130	.101	.117
6	.0967	.112	.035	.040	.107	.133	.101	.119
9	.0966	.101	.033	.036	.101	.121	.095	.107
3	.0651	.087	.024	.031	.0880*	.101	.082	.091
6	.0791	.094	.028	.033	.0928*	.108	.084	.097
9	.0821	.081	.028	.029	.0872*	.100	.080	.089

* Estimated from incomplete data

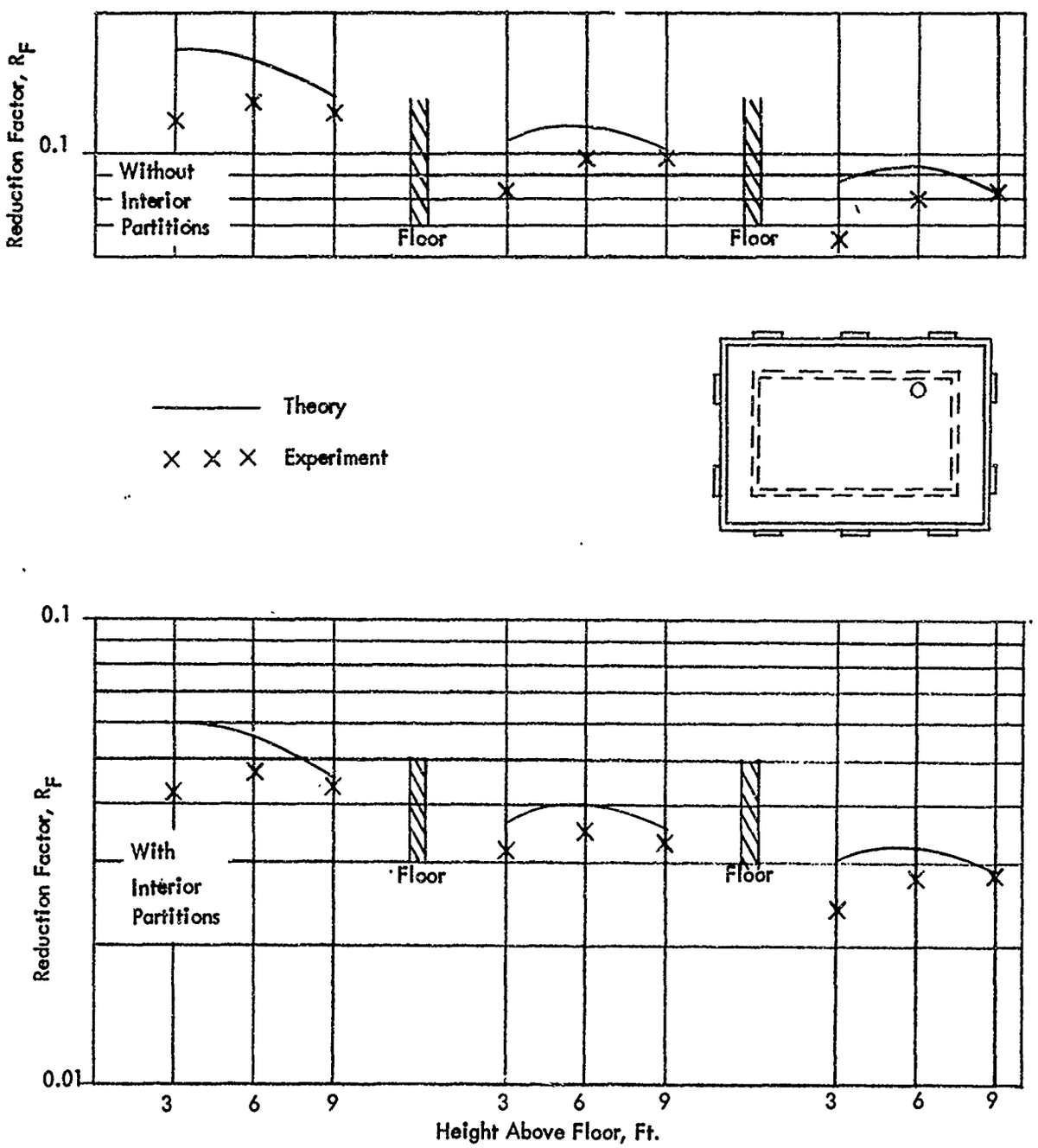

Figure 5.5 - Vertical Distribution of Reduction Factors at the (6, 9) Position of the Structure with Nonuniform Walls with and Without Interior Partitions

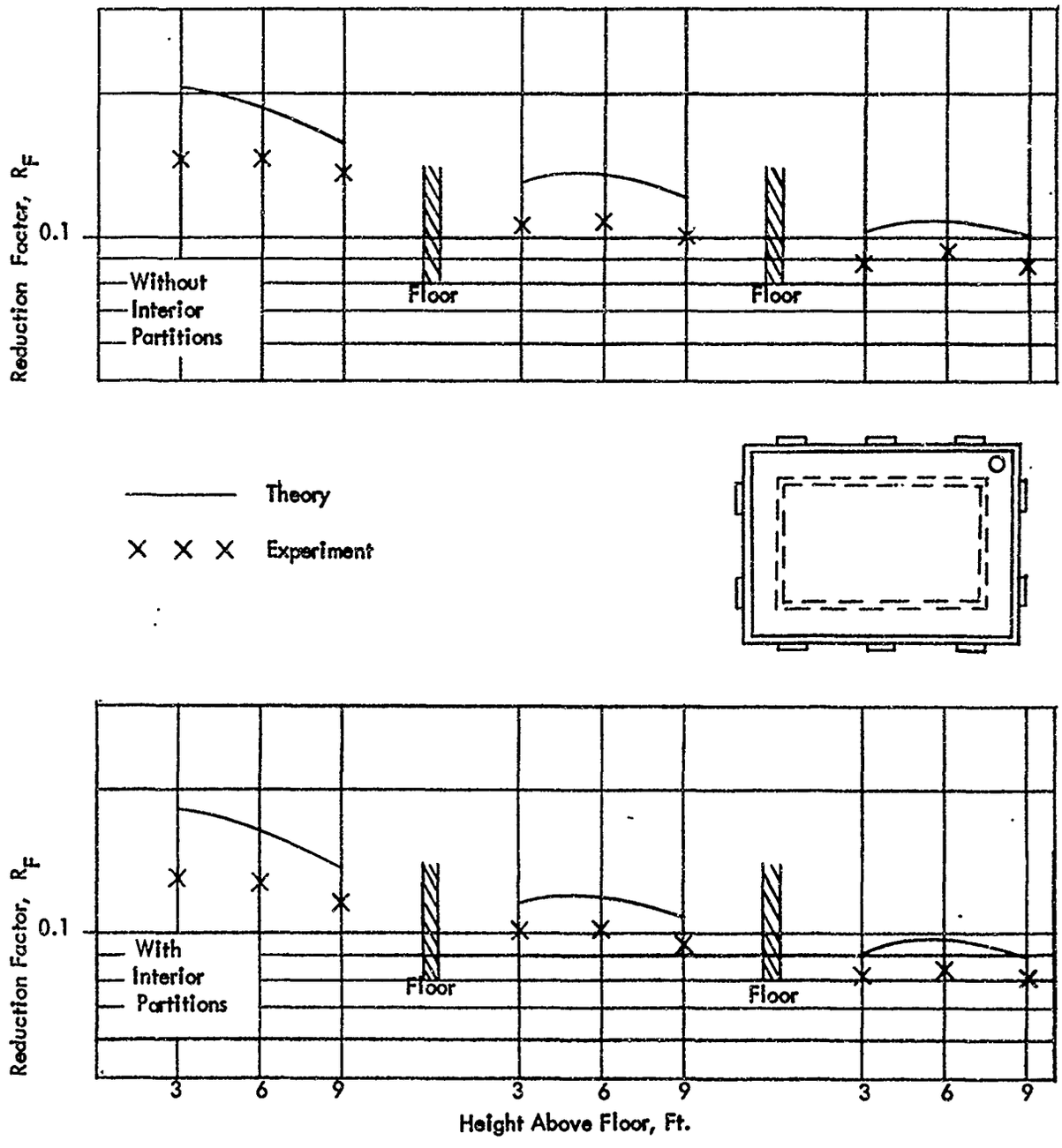

Figure 5.6 - Vertical Distribution of Reduction Factors at the (10, 15) Position of the Structure with Nonuniform Walls with and Without Interior Partitions

CHAPTER 6

CONCLUSIONS AND RECOMMENDATIONS

6.1 CONCLUSIONS

1. The experimental dose rates in the center of a structure with interior partitions increases as the partitions are moved toward the detector. In relation to the basic structure, in which all the mass is concentrated at the exterior wall, the increase in the dose rate, when the exterior wall mass is divided to form interior walls, is 15 percent when the interior walls are close to the exterior wall (Case 1, Configuration A) and 25 percent when the interior walls are concentrated near the detector (Case 2, Configuration A).

2. The reduction factors calculated for the structure with interior partition Configuration A, Case 1, are between 15 and 20 percent higher than experimental results for detector locations 3 feet above the floor.

3. The experimental reduction factors increase more rapidly with height above the floor than predicted by the calculations, possibly indicating that the scattered radiation emerging from the exterior walls, G_s, is not symmetrical with respect to the horizontal, as assumed in the calculations.

4. Comparing experimental and calculated results, we find good agreement (with foregoing qualifications) for the test structure with interior partition Configuration B.

5. The reduction factors calculated for the structure with apertures duplicate the general shape of the plot of the experimental results, but are conservative by as much as 30 percent.

6. The reduction factors calculated for the structure with apertures and interior partitions show the same trend as the experimental values but are less conservative than the results without the interior partitions. In locations below the sill height the calculations were slightly nonconservative.

7. For the structure with nonuniform exterior walls, the use of azimuthal sectors in the calculations appears to be valid. The agreement with experiment is about the same as that noticed for experiments with uniform exterior walls.

8. The presence of interior partitions in the structure with nonuniform exterior walls did not significantly alter the relative accuracy of the calculation technique.

9. The agreement between calculated and experimental results for off-center detector locations is about the same as that shown for centerline locations.

6.2 RECOMMENDATIONS

1. The wall scattered radiation term, G_s, is believed to be a major cause of discrepancies between theory and experiment at locations above mid-story height. These discrepancies, as shown in this study, can be as great as 30 percent with the theory underestimating the dose rate. The G_s function should be recalculated to determine the difference in wall scattered radiation from above and below the detector plane.

2. Further study, including experimental work on a structure with varying external wall thicknesses, should be undertaken to determine the effects of interior partitions on the dose rate in a structure with apertures.

REFERENCES

1. Auxier, J. A., Buchanan, J. O., Eisenhauer, C., and Menker, H. E., "Experimental Evaluation of the Radiation Protection Afforded by Residential Structures Against Distributed Sources," AEC Report CEX-58.1 (January 19, 1959).

2. Batter, J. F., Kaplan, A. L., and Clarke, E. T., "An Experimental Evaluation of the Radiation Protection Afforded by a Large Modern Concrete Office Building," CEX-59.1 (January 22, 1960).

3. OCD PM 100-1, "Design and Review of Structures for Protection from Fallout Gamma Radiation", (February 1965).

4. McDonnell, C. H., Velletri, J. Starbird, A. W., and Batter, J. F., "Description, Experimental Calibration, and Analysis of the Radiation Test Facility at the Protective Structures Development Center," PSDC-TR-14 (September 1964).

5. McDonnell, C. H., Velletri, J., Starbird, A. W., and Batter, J. F., "The Barrier Attenuation Introduced by a Vertical Wall," PSDC-TR-15 (September 1964).

6. McDonnell, C. H., and Velletri, J., "An Experimental Evaluation of Roof Reduction Factors," PSDC-TR-16 (May 1, 1966).

7. McDonnell, C. H., and Velletri, J., "Radiation Distribution Within a Multi-Story Structure," TR-24 (February 1967).

8. Spencer, L.V., "Structure Shielding Against Fallout Radiation from Nuclear Weapons," NBS Monograph 42 (June 1, 1962).

9. Velletri, J., "A Preliminary Investigation of 'In-and-Down' and 'In-and-Up' Radiation Components," PSDC-TR-25 (October 1966).

10. Eisenhauer, C., "An Engineering Method for Calculating the Protection Afforded by Structures Against Fallout Radiation," OCD PM-100-1 Supplement No. 1 (January 1964).

11. Kaplan, A. L., Waldman, J., Jones, J. L., Barch, W. E., and MacNeil, R. L., "Structure Shielding from Simulated Fallout Gamma Radiation," TO-B 65-27 (November 1965).

12. Starbird, A. W., Velletri, J., MacNeil, R. L., and Batter, J. F., "The Effect of Interior Partitions on the Dose Rate in a Multistory Windowless Building," TO-B 63-6 (January 1963).

APPENDIX A

DATA REDUCTION AND ANALYSIS

EXPERIMENTAL DATA

The experimental data reported in this study were obtained using Victoreen Model 362, 200-mR, Model 229, 10-mR, and Model 208, 1-mR non-direct reading ionization chambers (dosimeters) with a Technical Operations Model 556 Charger Reader. Chamber selection was based on the expected exposure time, the area of the field being simulated, the thickness of the walls, and the location of the dosimeter with respect to the contaminated area.

All chambers and the charger-reader were calibrated against a gamma source of known strength and National Bureau of Standards calibrated Victoreen R meters. Chambers which responded to within ± 2 percent of the known dose were selected for the experiment. The chambers were also checked at intervals during the experiment by a secondary calibration procedure.

Chambers were positioned at various heights at both centerline and off-center locations with respect to the simulated area of contamination. Off-center detector arrays were located at building co-ordinate positions (± 10, ± 15), (± 6, ± 9), (± 10, 0) and (± 6, 0). The convention used in assigning building coordinates is described in Fig. 2.3.

All detector readings were normalized to a specific dose rate; that is, to a per hour basis for an equivalent contamination density of one curie of Co-60 per square foot. This source density produced a radiation field of 464 R/hr 3 feet above an infinite, smooth, uniformly contaminated plane in an earlier experiment conducted at this facility. (Reference A-7). Detector readings were converted to R/hr using chamber calibration constants, exposure time, source strength, and temperature-pressure corrections for the effect of atmospheric conditions.

The experimental data of this study are tabulated in terms of the specific dose rate, i.e., roentgens per hour for a field density of one curie of Co-60 per square foot. These data for the full field of contamination are listed in Tables A-1 through A-4 for centerline positions and Tables A-5 through A-11 for off-center positions.

FAR FIELD CONTAMINATION

It is impossible to extend the simulated areas of contamination to infinite field conditions to permit direct comparisons with calculated results. An estimate of the dose that originates from areas of contamination in the "far field" (beyond the area simulated) must be added to the experimental data. Previous experiments have indicated that a field extending to about ten times the building height or one mean free path radius, whichever is greater, is sufficient to produce most of the dosage that would have been received from a truly infinite field, and that radiation arriving from beyond this radius would be attenuated by the structure in a manner

similar to that of the outermost annulus. This manner of attenuation results because the angular and energy distribution of radiation beyond one mean free path radius is nearly identical to that of the outermost annulus. Therefore, the method of estimation used for the effects of far field contamination is to multiply the dose measured within the structure from the outermost experimental annulus by the ratio of the free field dose originating beyond the outermost radius, divided by the free field dose from the outermost simulated contaminated area. The ratios needed for this procedure are presented in the following table as a function of height.

Ratio of "Far Field" Dose to That Obtained from the Experimental Area of Greatest Radius

Detector Height (ft)	Ratio	Detector Height (ft)	Ratio
1	0.567	21	0.574
3	0.568	24	0.575
6	0.569	27	0.576
9	0.570	30	0.577
12	0.571	33	0.578
15	0.572	36	0.579
18	0.573		

A more detailed description of this procedure is contained in Reference A-7.

INFINITE FIELD FREE FIELD DOSE RATES

In order to determine "reduction factors" from the experimental measurements the value of the dose rate above an infinite field of contamination must be ascertained. The methods of determining the value are:

1. Experimental "full field" measurements.
2. An integral over the uncollided radiation multiplied by a calculated infinite field plane buildup factor.
3. An integral over both the uncollided and scattered radiation, using either an experimental or analytical estimate of air over ground buildup factors.

Results of various investigations are illustrated in the table accompanying this Appendix. Some definitions and constants are needed, however, if all methods are to be compared under the same conditions. For this study standard conditions always refer to 0° C dry air at 760 mm Hg.

Definitions and Constants

Standard pressure	=	760 mm Gg
Standard temperature	=	0° C
Roentgen[1]	=	1.0 e.s.u. per .001293 g air
Electron volts per ion pair[2]	=	34.0
Average energy per photon Co-60	=	1.25 Mev
Total energy per disintegration[3] Co-60	=	2.505 Mev
Mass energy absorption cross section[4] for air at 1.25 Mev	=	0.0267 cm^2/g
Density of dry air at STP	=	0.001293 g/cm^3
"q" = specific dose rate	=	14.0 R/hr at 1 ft for 1 Curie of Co-60

This value of "q" for Co-60 radiation is computed as follows:

$$q = \frac{(3.7 \times 10^{10})\ (2.505)\ (3600.)\ (0.0267)}{(4\pi)\ \left(\frac{1}{.001293}\right)\ (2.082 \times 10^{9})\ (34.0 \times 10^{-6})\ (10^{4})} = 1.295 \text{ R/hr at 1 meter}$$

The dimensional analysis of this calculation is:

$$\frac{\text{R/hr}}{\text{curie/ meter}} = \frac{\frac{\text{dps}}{\text{curie}}\ \frac{\text{Mev}}{\text{dis.}}\ \frac{\text{sec}}{\text{hr}}\ \frac{\text{cm}^2}{\text{g}}}{\frac{\text{e.s.u.}}{\text{R - g}}\ \frac{\text{ion pair}}{\text{e.s.u.}}\ \frac{\text{Mev}}{\text{ion pair}}\ \frac{\text{cm}^2}{\text{m}^2}}$$

Thus, one curie of cobalt radiation produces 1.295 roentgens per hour at a distance of one meter or 13.94 roentgens per hour at one foot. This value is commonly rounded off, for convenience, to 14.0 (R/hr)/ft.

Infinite Field Dose Rate at 3' Altitude
and STP above a Field of One Curie
per Square Foot Cobalt - 60

Report Reference	Method	Buildup Factor	Value (R/hr)
A-5	Experimental		487
A-6	Linear buildup factor	$B(\mu x) = 1 + 0.55 \mu x$	438
A-7	Experimental	-------	464
A-8	Experimental	-------	480
A-9	Plane buildup factor	B (3') = 1.208	471
A-10	Plane buildup factor	B (3') = 1.220	475
A-11	Plane buildup factor	B (3') = 1.171	456
A-12	Plane buildup factor	B (3') = 1.195	466
A-13	Linear buildup factor	$B(\mu x) = 1.0 + 0.95 \mu x^{0.061 \mu x}$	470*
A-14	Experimental	-------	458

* Corrected for error in definition of a roentgen

The value of infinite field dose rate at the 3 foot height in this study is taken as 464 (R/hr)/(curie/ft^2) of Co-60 which is consistent with both the value measured (see third entry of table) at the RTF and those measured and calculated by other investigators when the values are reduced to common conditions.

TABLE A-1
SPECIFIC DOSE RATES
CENTERLINE LOCATION
INTERIOR PARTITIONS - CONFIGURATION A
(R/hr)/(Ci/ft^2)

HEIGHT ABOVE FLOOR SURFACE (FT)	CASE 1 FIELD RADIUS (FT) 0-32	32-68	68-164	164-452	CASE 2 FIELD RADIUS (FT) 0-32	32-68	68-164	164-452
FIRST STORY								
1	4.40	5.32	5.12	3.52	4.88	6.24	5.84	3.80
2	5.20	6.12	5.96	4.24	6.64	7.20	7.04	4.80
3	5.56	6.48	6.52	4.72	6.96	7.68	7.52	5.48
4	5.72	6.68	6.88	5.00	7.04	7.96	8.04	6.00
5	5.68	6.80	7.12	5.28	7.00	8.04	8.72	6.40
6	5.64	6.88	7.28	5.40	6.88	8.36	8.68	6.56
7	5.52	6.92	7.32	5.44	6.60	8.36	8.60	6.72
8	5.24	6.92	7.20	5.36	6.32	8.08	8.40	6.60
9	4.96	6.88	6.84	5.24	5.84	7.68	8.24	6.36
SECOND STORY								
1	0.306	1.60	3.20	4.72	0.312	1.28	2.78	5.24
2	0.341	1.88	5.24	5.76	0.316	1.50	5.52	7.12
3	0.364	2.25	6.36	6.04	0.326	1.84	6.96	7.40
4	0.394	2.72	7.12	6.16	0.340	2.66	7.84	7.60
5	0.420	3.26	7.36	6.24	0.376	3.40	8.36	7.72
6	0.452	3.72	7.48	6.20	0.412	4.00	8.64	7.76
7	0.484	4.08	7.44	6.16	0.448	4.44	8.68	7.72
8	0.520	4.28	7.32	6.08	0.520	4.76	8.60	7.56
9	0.560	4.36	7.12	5.92	0.568	4.84	8.48	7.32
10	0.608	4.24	6.80	5.76	0.624	4.72	7.84	6.72
THIRD STORY								
1	0.0652	0.672	2.00	3.40	0.0808	0.640	1.81	2.90
2	0.0728	0.788	2.64	5.16	0.0720	0.580	2.24	5.56
3	0.0792	0.846	3.40	5.72	0.0724	0.700	3.36	6.88
4	0.0848	1.00	4.28	5.92	0.0804	0.756	4.68	7.36
5	0.0888	1.12	5.12	6.12	0.0840	0.872	5.68	7.52
6	0.0924	1.24	5.52	6.16	0.0872	1.14	6.32	7.68
7	0.0952	1.36	5.84	6.20	0.0900	1.28	6.88	7.72
8	0.0980	1.50	6.04	6.20	0.0916	1.57	7.16	7.72
9	0.100	1.66	6.16	6.08	0.0916	1.71	7.20	7.52
10	0.102	1.83	6.16	4.92	0.0892	1.74	7.12	7.16

TABLE A-2
SPECIFIC DOSE RATES
CENTERLINE LOCATION
INTERIOR PARTITIONS - CONFIGURATION B
$(R/hr)/(Ci/ft^2)$

HEIGHT ABOVE FLOOR SURFACE (FT)	FIELD RADIUS (FT)			
	0-32	32-68	68-164	164-452
FIRST STORY				
1	9.12	9.28	8.56	5.64
2	9.88	10.12	9.68	6.72
3	10.32	10.76	10.48	7.44
4	10.68	11.24	11.12	7.88
5	10.72	11.52	11.52	8.16
6	10.56	11.60	11.72	8.36
7	10.32	11.52	11.80	8.52
8	10.00	11.28	11.72	8.52
9	9.64	11.04	11.52	8.48
SECOND STORY				
1	.552	2.20	4.32	8.00
2	.620	2.52	8.32	9.20
3	.680	3.16	10.88	9.68
4	.732	4.60	11.52	9.92
5	.792	5.80	11.84	10.08
6	.848	6.64	12.00	10.00
7	.924	7.16	12.04	9.88
8	1.03	7.48	12.00	9.68
9	1.17	7.52	11.92	9.40
10	1.40	7.40	11.68	9.08
THIRD STORY				
1	0.150	1.14	3.29	4.72
2	0.157	1.31	3.74	8.16
3	0.166	1.47	5.52	9.24
4	0.176	1.59	6.72	9.64
5	0.192	1.68	8.36	9.84
6	0.204	2.04	9.20	9.88
7	0,216	2.50	9.80	9.88
8	0.224	2.92	10.08	9.88
9	0.228	3.20	10.08	9.88
10	0.232	3.40	10.00	9.88

TABLE A-3
SPECIFIC DOSE RATES
CENTERLINE LOCATION
APERTURES - WITH AND WITHOUT INTERIOR PARTITIONS
(R/hr)/(Ci/ft^2)

HEIGHT ABOVE FLOOR SURFACE (FT)	0 PSF INTERIOR PARTITION FIELD RADIUS (FT)				42 PSF INTERIOR PARTITION FIELD RADIUS (FT)			
	0-32	32-68	68-164	164-452	0-32	32-68	68-164	164-452
FIRST STORY								
1	10.52	15.60	12.28	9.32	5.48	6.48	6.60	4.08
2	13.16	16.60	15.20	11.44	6.00	7.12	6.64	4.80
3	14.00	17.28	16.16	12.32	6.44	7.68	7.04	5.16
4	14.44	17.32	16.52	13.08	6.72	8.04	7.40	6.00
5	14.52	16.44	23.40	24.00*	6.84	8.36	9.80	8.52
6	14.40	19.88	30.28	25.28	6.64	9.00	11.68	9.52
7	14.28	26.84	31.36	25.44	6.48	10.80	12.36	9.44
8	14.52	29.52	31.92	25.44	6.52	11.68	11.76	9.28
9	14.72	30.30	28.56	12.40	6.60	11.80	10.40	6.00
SECOND STORY								
1	0.832	3.34	6.00*	13.52	0.336	1.80	3.68	5.28
2	0.888	3.90	11.60	14.40*	0.370	2.08	5.80	6.12
3	0.964	4.64	15.16	15.28	0.404	2.44	6.68	6.44
4	1.05	6.40	17.16	15.60	0.436	2.87	7.36	6.68
5	1.14	8.08	16.52	16.00	0.468	3.52	7.88	6.92
6	1.28	9.28	18.60	26.56	0.500	4.28	8.16	10.32
7	1.42	10.96	22.20	28.00	0.528	4.52	9.76	10.64
8	1.56	11.48	26.60	28.12	0.576	4.64	10.84	10.36
9	1.70	12.48	29.88	27.64	0.616	5.00	11.52	9.74
10	1.86	16.20	31.32	18.28	0.672	5.32	11.84	7.00
THIRD STORY								
1	0.229	1.80	4.28	6.76	0.0776	0.884	2.86	4.60
2	0.255	2.00	5.28	14.40	0.0812	0.960	3.40	6.20
3	0.280	2.20	7.60	16.20	0.0860	1.10	4.36	7.32
4	0.302	2.34	10.28	17.32	0.0984	1.22	5.72	7.80
5	0.320	2.52	14.32	16.56	0.106	1.32	6.52	8.16
6	0.348	3.09	15.60*	30.00*	0.112	1.43	7.20	10.28
7	0.358	3.62	15.64	44.80	0.115	1.83	7.80	15.40
8	0.361	4.24	22.92	48.40	0.117	2.02	9.80	18.12
9	0.372	4.60	29.88	49.20	0.118	2.20	12.04	17.24
10	0.368	5.16	39.08	42.00	0.114	2.36	14.40	14.60

* Estimated Values

TABLE A-4
SPECIFIC DOSE RATES
CENTERLINE LOCATION
NONUNIFORM WALLS-
WITH AND WITHOUT INTERIOR PARTITIONS
$(R/hr)/(Ci/ft^2)$

HEIGHT ABOVE FLOOR SURFACE (FT)	0 PSF INTERIOR PARTITION FIELD RADIUS (FT)				42 PSF INTERIOR PARTITION FIELD RADIUS (FT)			
	0-32	32-68	68-164	164-452	0-32	32-68	68-164	164-452
FIRST STORY								
1	8.76	11.60	10.92	6.68	3.40	4.36	4.28	2.70
2	10.48	12.48	11.76	8.16	4.16	4.64	4.56	3.26
3	11.40	13.04	12.72	8.96	4.40	4.84	4.88	3.61
4	11.52	13.44	13.36	9.52	4.48	4.96	5.12	3.90
5	11.56	13.68	13.60	10.04	4.44	5.08	5.32	4.08
6	11.60	13.92	13.76	10.28	4.36	5.12	5.44	4.16
7	11.48	13.96	13.80	10.32	4.28	5.12	5.48	4.16
8	11.08	13.92	13.84	10.36	4.08	5.08	5.36	4.12
9	10.20	13.80	13.80	10.32	3.80	5.04	4.72	4.00
SECOND STORY								
1	0.628	2.82	5.20	9.60	0.218	1.40	2.50	3.65
2	0.652	3.20	8.84	11.48	0.242	1.40	3.85	4.48
3	0.720	3.74	12.68	12.16	0.270	1.60	4.64	4.64
4	0.780	5.08	14.20	12.44	0.294	2.11	5.00	4.76
5	0.844	6.16	14.48	12.48	0.318	2.51	5.12	4.84
6	0.884	7.52	14.56	12.44	0.342	2.81	5.28	4.88
7	0.972	8.96	14.56	12.40	0.364	3.01	5.36	4.84
8	1.11	9.44	14.48	12.28	0.386	3.11	5.32	4.76
9	1.22	9.52	14.32	12.20	0.408	3.19	5.20	4.64
10	1.24	9.12	14.16	12.12	0.432	3.11	4.80	4.48
THIRD STORY								
1	0.176	1.36	4.16	5.48	0.0476	0.500	1.68	2.74
2	0.176	1.52	4.60	10.12	0.0508	0.552	2.08	4.00
3	0.178	1.68	6.64	11.92	0.0528	0.628	2.65	4.60
4	0.192	1.84	8.56	12.08	0.0584	0.704	3.36	4.76
5	0.204	1.99	10.12	12.52	0.0624	0.780	3.80	4.84
6	0.207	2.34	11.40	13.00	0.0664	0.896	4.16	4.88
7	0.218	2.70	12.28	13.28	0.0700	1.01	4.48	4.84
8	0.226	3.08	12.76	12.88	0.0700	1.12	4.60	4.76
9	0.234	3.49	12.96	12.48	0.0720	1.19	4.56	4.64
10	0.239	3.79	13.08	13.00	0.0700	1.22	4.28	4.52

TABLE A-5
SPECIFIC DOSE RATES
OFF-CENTER LOCATIONS
INTERIOR PARTITIONS - CONFIGURATION A, CASE 1
$(R/hr)/(Ci/ft^2)$

Position	Field Radius (FT)		DETECTOR HEIGHT ABOVE FLOOR SURFACE (FT)								
			First Story			Second Story			Third Story		
			3	6	9	3	6	9	3	6	9
10, 15	0	32	20.18	15.60	9.36	2.88	2.53	1.89	0.544	0.583	0.473
	32	68	19.25	19.11	18.21	13.68	12.68	11.58	7.09	6.89	6.13
	68	164	15.40	17.22	16.83	16.73	17.34	16.74	15.01	15.69	15.02
	164	452	9.64	12.10	12.37	14.43	15.35	13.89	14.07	15.93	13.50
6, 9	0	32	6.84	6.13	4.89	0.434	0.690	0.640	0.116	0.127	0.149
	32	68	6.93	7.33	7.03	3.33	4.37	4.79	1.11	1.72	2.06
	68	164	6.68	7.45	7.17	6.63	7.44	7.09	4.63	5.71	5.98
	164	452	4.39	5.03	5.21	6.09	6.59	5.91	5.78	6.15	6.26
0, 15	0	32	12.62	11.24	7.80	1.36	1.49	1.29	0.248	0.260	0.244
	32	68	13.40	14.42	12.40	9.02	9.84	8.86	4.20	4.64	4.58
	68	164	11.40	12.90	12.02	12.88	13.36	13.00	10.76	11.56	11.48
	164	452	7.74	9.72	9.02	11.08	12.74	10.40	10.66	12.50	10.16
0, 9	0	32	5.94	5.82	5.04	0.380	0.492	0.648	0.080	0.095	0.100
	32	68	7.20	7.38	7.14	2.74	4.32	4.74	0.097	1.53	1.90
	68	164	6.62	7.50	7.04	6.88	7.74	7.40	4.26	6.14	6.14
	164	452	4.60	5.62	4.98	6.08	6.66	6.40	5.84	6.44	6.80
10, 0	0	32	15.84	12.54	10.18	2.61	2.19	1.75	0.520	0.528	0.432
	32	68	12.40	12.94	12.14	8.28	8.50	8.08	4.68	4.50	4.46
	68	164	11.46	12.08	12.16	11.88	12.32	12.36	9.46	11.04	10.38
	164	452	8.38	8.82	10.76	10.56	10.62	10.54	9.72	10.62	10.22
6, 0	0	32	6.30	5.84	4.72	0.408	0.634	0.592	0.087	0.100	0.112
	32	68	6.56	7.20	6.56	2.94	3.78	3.96	0.990	1.52	1.69
	68	164	6.54	6.92	6.76	5.94	7.06	7.06	3.94	5.20	5.68
	164	452	4.56	5.12	5.02	5.78	6.00	5.70	5.48	5.82	5.64

TABLE A-6
SPECIFIC DOSE RATES
OFF-CENTER LOCATIONS
INTERIOR PARTITIONS - CONFIGURATION B
(R/hr)/(Ci/ft^2)

Position	Field Radius (ft)	DETECTOR HEIGHT ABOVE FLOOR SURFACE (FT)								
		First Story			Second Story			Third Story		
		3	6	9	3	6	9	3	6	9
10, 15	0 32	24.66	16.09	11.38	2.78	2.48	1.90	.535	.568	.504
	32 68	21.01	21.14	19.80	14.15	13.53	12.15	-----	7.43	6.40
	68 164	16.20	18.12	-----	-----	-----	-----	-----	-----	-----
	164 452	-----	-----	-----	-----	-----	-----	-----	-----	-----
6, 9	0 32	15.29	13.96	11.82	1.03	1.56	1.71	.251	.294	3.43
	32 68	15.31	16.44	15.56	7.38	10.02	10.45	-----	4.66	-----
	68 164	-----	-----	-----	-----	-----	-----	-----	-----	-----
	164 452	-----	-----	-----	-----	-----	-----	-----	-----	-----
0, 15	0 32	20.44	15.96	11.76	1.34	1.60	1.72	.266	.328	3.26
	32 68	16.84	17.78	17.02	9.18	11.18	10.76	-----	5.12	5.66
	68 164	-----	-----	-----	-----	-----	-----	-----	-----	-----
	164 452	10.06	11.84	11.64	-----	-----	-----	-----	-----	-----
0, 9	0 32	13.90	12.94	11.60	.790	1.00	1.33	.198	.230	.250
	32 68	15.12	15.76	15.52	5.18	9.62	10.44	1.95	3.28	4.74
	68 164	-----	-----	-----	-----	-----	-----	-----	-----	-----
	164 452	-----	-----	-----	-----	-----	-----	-----	-----	-----
10, 0	0 32	17.44	12.94	10.70	2.88	2.40	1.89	.538	.558	.474
	32 68	13.36	13.70	13.50	8.30	8.44	8.42	4.68	4.64	4.22
	68 164	13.08	13.84	13.42	12.44	14.10	13.74	-----	11.54	11.94
	164 452	8.74	10.26	10.32	11.14	11.42	11.08	10.78	11.68	11.50
6, 0	0 32	12.68	11.86	10.00	.962	1.67	1.70	.228	.286	.354
	32 68	11.78	12.16	11.98	5.70	7.14	5.84	1.96	3.36	3.78
	68 164	11.12	11.98	11.92	10.68	12.46	11.98	7.60	9.96	10.62
	164 452	7.54	9.44	9.20	10.06	10.70	10.14	10.02	10.70	10.78

TABLE A-7
SPECIFIC DOSE RATES
(10, 0) LOCATION
APERTURES - WITH AND WITHOUT INTERIOR PARTITIONS
(R/hr)/(Ci/ft^2)

HEIGHT ABOVE FLOOR SURFACE (FT)	0 PSF INTERIOR PARTITION FIELD RADIUS (FT)				42 PSF INTERIOR PARTITION FIELD RADIUS (FT)			
	0-32	32-68	68-164	164-452	0-32	32-68	68-164	164-452
FIRST STORY								
1	16.96	14.90	12.74	7.66	17.54	11.68	8.80	6.42
2	18.04	16.56	14.82	10.98	18.18	11.78	10.76	8.10
3	18.48	17.10	15.78	12.86	17.08	13.70	11.76	9.46
4	17.14	16.24	16.62	15.02	15.78	13.76	12.54	10.60
5	22.84	26.76	28.00	27.80	19.60	25.48	22.50	18.08
6	25.58	27.72*	34.02	28.06	22.70	25.98	23.30	18.80
7	26.82	29.06	35.24	27.98	23.90	26.68	23.30	18.68
8	25.98	30.20	32.56	20.64	22.48	26.26	23.16	13.20
9	23.26	21.80	22.68	14.40	19.06	14.64	12.44	10.00
10	16.86*	21.80	22.12	13.24	13.24	14.20	11.36	9.52
SECOND STORY								
1	1.53	6.32	10.76	8.94*	1.61	7.00	10.22	9.16
2	2.54	8.30	11.84	11.62	2.60	10.60	11.08	10.40
3	2.80	8.60	14.36	15.18	2.92	9.28	12.24	11.04
4.3	2.76	9.06	15.86*	16.44	2.78	8.10	13.62	11.56
5.3	2.58	9.26	26.60	26.06	2.62	9.86	26.16	21.62
6.3	2.40	16.46	28.44	28.54	2.44	19.68	26.50	22.82
7.3	4.66	16.60	29.66	30.56	4.84	20.04*	26.60	21.98
8.3	5.38	16.56	29.78	29.54	5.78	20.18	26.62	19.90
9.3	5.80	17.20	22.66	20.30	6.24	19.82	14.00	10.92
10.3	5.96	17.70*	24.88	15.08	6.20	20.28	13.38	10.22
THIRD STORY								
3	0.620	4.92	11.00	15.50	0.670	4.82	9.26	10.98
4.3	0.658	5.30*	12.48	17.36	0.698	5.30	10.04	12.70
6	0.648	6.78	26.36	34.30	0.680	6.28	26.84	27.76
9	1.79	14.36	31.14	34.16	1.73	16.04	26.82	17.48

* Estimated Values

TABLE A-8
SPECIFIC DOSE RATES
OFF-CENTER LOCATIONS
STRUCTURE WITH APERTURES
$(R/hr)/(Ci/ft^2)$

Position	Field Radius (Ft)		DETECTOR HEIGHT ABOVE FLOOR SURFACE (FT)								
			First Story			Second Story			Third Story		
			3	6	9	3	6	9	3	6	9
10, 15	0	32	21.68	22.23	21.20	2.88	2.57	4.39	0.635	0.687	1.50
	32	68	19.86	30.71	25.41	13.37	16.10	19.03	7.30	7.29	23.58
	68	164	17.14	29.50	21.18	17.64	27.42	25.17	14.72	37.97	40.68
	164	452	11.68	25.13	16.09	14.47	22.74	17.04	17.29	42.51	26.03
6, 9	0	32	16.55	15.64	17.04	1.38	2.05	3.11	0.366	0.435	0.501
	32	68	17.09	26.32	30.73	7.81	11.06	8.51	3.63	4.96	8.03
	68	164	15.68	29.48	23.20	15.42	21.87	29.66	10.92	15.74	32.61*
	164	452	12.28	23.51	12.74	15.27	23.90	21.24	15.84	35.27	44.66
0, 15	0	32	18.26	15.32	16.90	1.62	1.80	1.91	0.346	0.432	0.464
	32	68	17.18	27.54	31.28	9.90	11.96	16.12	4.40	5.22	14.06
	68	164	15.66	26.98	23.16	19.64	20.06	28.06	11.90	23.96	34.22
	164	452	12.32	23.42	17.60	15.02	23.32	21.26	15.32	37.86	36.30
0, 9	0	32	15.48	17.32	16.08	1.48	1.38	1.88	0.278	0.352	0.384
	32	68	17.26	24.98	31.14	5.86	11.38	15.86	3.16	9.14	15.60
	68	164	15.72	30.56	23.84	16.20	19.82	23.74	4.54	15.50	29.64
	164	452	12.48	24.08	14.14	15.70	24.62	24.64	7.04	35.08	48.24
6, 0	0	32	15.80	16.18	17.48	1.25	1.93	2.02	0.376	0.422	0.472
	32	68	16.02	22.56	29.96	8.30	9.54	15.02	2.30	3.90	6.14
	68	164	16.38	28.88	26.56	14.80	21.76	28.82	9.40	15.06	11.90
	164	452	11.88	24.92	13.82	13.08	22.81	22.58	15.00	30.24	48.00

* Estimated Values

TABLE A-9
SPECIFIC DOSE RATES
OFF-CENTER LOCATIONS
STRUCTURE WITH APERTURES AND INTERIOR PARTITIONS
$(R/hr)/(Ci/ft^2)$

Position	Field Radius (ft)		DETECTOR HEIGHT ABOVE FLOOR SURFACE (FT)								
			First Story			Second Story			Third Story		
			3	6	9	3	6	9	3	6	9
10, 15	0	32	21.33	23.14	20.92	3.05	2.67	4.94	0.668	2.42	1.53
	32	68	21.49	30.00	22.34	14.65	17.42*	20.49	7.19	8.22	24.91
	68	164	15.36	25.26	16.75	17.83	28.07	23.02	14.37	37.02	30.34
	164	452	12.23	20.76	13.80	14.61	22.52	14.49	14.91	40.79	19.41
6, 9	0	32	7.51	7.10	7.08	0.605	0.718	0.674	0.108	0.123	0.131
	32	68	8.38	11.95	13.57	3.61	3.68	4.16*	1.25	1.90	2.01
	68	164	7.12	12.14	9.53*	7.46	10.52	11.71	5.40	7.90	13.68*
	164	452	5.26	9.55	6.30	6.55	10.02	9.86	6.78	13.53	15.07
0, 15	0	32	16.00	12.76	11.32	1.44	1.52	1.25	0.252	0.300	0.336
	32	68	15.70	21.88	21.08	9.36	10.20	12.44	4.20	5.00	13.64
	68	164	11.64	18.08	12.80	14.14	18.04	19.38	8.92	22.48	35.88
	164	452	9.24	12.70	11.12	10.48	16.32	12.40	11.80	31.60	21.86
0, 9	0	32	7.10	6.96	.64	0.452	0.562	0.600	0.087	0.107	0.116
	32	68	8.08	10.86	12.46	2.96	4.80	5.78	1.18	1.87	2.48
	68	164	7.74	11.58	11.04	7.58	9.16	11.72	5.02	8.10	13.76
	164	452	5.72	10.02	6.62	7,62	9.12	10.36	7.08	12.10	17.16
6, 0	0	32	7.32	7.12	7.14	1.67	2.06	2.30	0.370	0.404	0.454
	32	68	7.36	10.40	12.02	3.22	4.26	5.80	1.14	1.68	2.78
	68	164	7.18	12.12	10.18	7.18	10.56	12.12	4.60	7.14	12.02
	164	452	5.48	10.00	6.32	6.36	9.38	7.98	6.28	11.62	15.14

* Estimated Values

TABLE A-10
SPECIFIC DOSE RATES
OFF-CENTER LOCATIONS
STRUCTURE WITH NONUNIFORM WALLS
(R/hr)/(Ci/ft^2)

Position	Field Radius (Ft)	DETECTOR HEIGHT ABOVE FLOOR SURFACE (FT)								
		First Story			Second Story			Third Story		
		3	6	9	3	6	9	3	6	9
10, 15	0 32	17.07	13.49	9.19	1.98	1.73	1.32	0.334*	0.344*	0.276*
	32 68	18.47	18.70	17.18	11.66	10.88	9.51	6.11	5.56	4.98
	68 164	15.59	16.59	16.51	14.81	16.16	15.94	12.58	13.79	13.41
	164 452	10.14	11.69	12.25	12.72	13.38	12.87	13.85	14.82	13.82
6, 9	0 32	13.16	12.26	10.26	0.898	1.39	1.47	0.214	0.260	0.316
	32 68	13.82	15.02	14.45	6.28	8.75	9.10	2.30	3.77	4.26
	68 164	13.55	14.93	14.54	12.65	14.94	14.73	8.88	11.71	12.60
	164 452	9.31	10.59	10.80	12.03	12.58	12.39	11.94	13.29	13.27
0, 15	0 32	16.22	11.50	10.28	1.30	1.48	1.44	0.174*	0.214*	0.204*
	32 68	15.62	16.54	15.82	9.18	10.72	9.98	3.78	4.60	4.96
	68 164	13.84	15.08	14.56	14.16	15.48	15.66	10.80	12.92	12.50
	164 452	9.60	11.14	11.12	12.54	12.82	12.60	12.64	13.12	13.58
0, 9	0 32	12.46	12.08	11.30	5.78	7.00	9.78	0.177	0.210	0.228
	32 68	14.20	15.28	14.70	4.76	9.00	9.38	1.82	3.00	4.38
	68 164	13.46	14.72	14.30	13.12	14.56	14.80	7.96	10.70	11.22
	164 452	9.16	10.22	10.06	11.80	12.50	12.00	12.14	12.96	13.40
10, 0	0 32	11.34	9.82	7.76	.780	.766	1.09	0.232	0.256	0.224
	32 68	12.08	12.30	11.72	5.28	5.86	6.68	2.85	2.96	2.94
	68 164	11.08	12.10	11.58	10.14	12.04	12.08	6.74	9.20	10.30
	164 452	6.66	9.46	9.30	9.80	10.36	10.06	10.40	10.96	11.54
6, 0	0 32	11.54	12.40	10.84	0.874	1.33	1.33	0.189	0.220	0.280
	32 68	13.48	14.86	14.48	4.38	7.24	8.48	1.87	3.18	3.48
	68 164	13.08	14.34	14.16	11.70	13.98	13.58	7.44	10.72	12.40
	164 452	8.56	9.90	10.30	11.36	12.00	11.82	12.52	13.26	12.96

* Estimated Values

TABLE A-11
SPECIFIC DOSE RATES
OFF-CENTER LOCATIONS
STRUCTURE WITH NONUNIFORM WALLS AND INTERIOR PARTITIONS
(R/hr)/(Ci/ft^2)

Position	Field Radius (Ft)		DETECTOR HEIGHT ABOVE FLOOR SURFACE (FT)								
			First Story			Second Story			Third Story		
			3	6	9	3	6	9	3	6	9
10, 15	0	32	15.85	10.84	7.10	1.97	1.69	1.19	0.352	0.360	0.283
	32	68	17.15	16.59	15.31	11.43	10.56	9.19	5.56	5.57	5.38
	68	164	13.24	14.67	14.37	14.09	14.57	13.79	12.13	12.68	11.93
	164	452	9.06	10.95	11.43	12.47	12.73	12.57	12.56	12.90	12.43
6, 9	0	32	4.36*	4.49*	3.59	0.318	0.500	0.468	0.062	0.074	0.083
	32	68	5.23	5.39	5.18	2.44	3.05	3.07	0.772	1.20	1.41
	68	164	4.70	5.23	5.10	4.81	5.10	5.06	3.31	4.15	4.13
	164	452	3.58*	4.14	4.04	4.56	4.82	4.37	4.33	4.80	4.60
0, 15	0	32	14.20	10.24	7.52	0.984	1.17	1.00	0.174	0.216	0.202
	32	68	12.70	13.10	11.92	7.84	8.32	7.64	4.58	4.18	3.68
	68	164	10.28	11.28	10.70	11.24	11.34	11.40	8.96	10.20	9.94
	164	452	7.18	9.20	9.28	9.74	10.28	9.46	9.96	10.44	10.44
0, 9	0	32	5.00	4.78	3.90	0.280	0.362	0.456	0.058	0.068	0.072
	32	68	5.42	5.68	5.52	1.91	3.26	3.66	0.698	1.36	1.29
	68	164	4.78	5.32	5.06	4.92	5.66	5.12	3.08	4.34	4.40
	164	452	3.60	3.82	3.98	4.72	5.06	4.66	4.58	4.82	4.84
10, 0	0	32	7.68	7.12	5.36	1.18	0.984	0.742	0.326	0.228	0.206
	32	68	7.74	8.04	7.86	4.44	4.46	4.50	2.12	2.10	2 12
	68	164	6.88	7.20	7.12	6.78	7.30	7.14	5.30	6.18	6.38
	164	452	4.50	5.36	6.04	6.36	6.44	6.76	5.84	6.60	6.72
6, 0	0	32	4.68	4.26	3.40	0.306	0.428	0.410	0.058	0.066	0.072
	32	68	4.68	5.26	4.82	2.08	2.64	2.84	0.670	0.982	1.17
	68	164	4.60	4.60	4.74	4.28	5.00	6.60	2.74	3.60	3.92
	164	452	3.36	3.94	3.88	4.40	4.62	4.32	4.16	4.46	4.34

* Estimated Values

REFERENCES FOR APPENDIX

A-1 "International Recommendation on Radiological Units 1953", Radiology 62, 106 (1954)

A-2 "Report of the International Commission on Radiological Units and Measurements", NBS Handbook 62 (1957)

A-3 Review of Modern Physics 30 631 (1958)

A-4 "Report of the International Commission on Radiological Units and Measurements," NBS Handbook 78 (1959)

A-5 "Scattered Radiation and Free Field Dose Rate from Distributed Cobalt-60 and Cesium-137 Sources", Rexroad, R. E. and Schmoke, M. A. NDL - TR - 2 (September 1960)

A-6 "Measurement of Attenuation in Existing Structures of Radiation from Simulated Fallout", Clarke, E. T., Batter, J. F., and Kaplan, A. L., TO-B 59-4 (April 27, 1959)

A-7 "Description, Experimental Calibration, and Analysis of the Radiation Test Facility at the Protective Structures Development Center", McDonnell, C. H., Velletri, J., Starbird, A. W., and Batter, J. F., PSDC-TR-14 (September 1, 1964)

A-8 "Measurements of Gamma Radiation and Gamma Spectra Versus Height Above a Fallout Simulated with Co-60", NDL-TR-70 (1965)

A-9 "Structure Shielding Against Fallout Radiation from Nuclear Weapons", Spencer, L. V., NBS Monograph 42 (June 1962)

A-10 Journal of Applied Physics, Berger, M. (1957)

A-11 "Simulation of Fallout Gamma Radiation Fields by Monoenergetic Plane Isotropic Sources", RRA - M51, French, R. L.

A-12 "Comparison of Monte Carlo Calculations with Experimental Results for the Propagation of Gamma Rays Near an Air-Ground Interface", RM 3399 PR (1962)

A-13 "Scattering of Fallout Radiation from Ceilings of Protective Structures," Kimel, W. R., Faw, R. E., Baran, J. A., Mingle, J. O., Rubin, R. M., Iotti, R. C., Urban. W. T., KSU Special Report Number 72 (July 1966)

A-14 "Scattered Radiation (Skyshine) Contribution to an Open Basement Located in a Simulated Fallout Field", Schumchyk, M. J., Schmoke, M. A., Egerland, W. O., Schulman, E.L., NDL - TR - 68 (December 66)

UNCLASSIFIED

Security Classification

DOCUMENT CONTROL DATA - R & D

(Security classification of title, body of abstract and indexing annotation must be entered when the overall report is classified)

1. ORIGINATING ACTIVITY (Corporate author)	2a. REPORT SECURITY CLASSIFICATION
Radiation Test Facility Fort Belvoir, Virginia	UNCLASSIFIED
	2b. GROUP

3. REPORT TITLE

EXPERIMENTAL ANALYSIS OF INTERIOR PARTITIONS, APERTURES AND NONUNIFORM WALLS

4. DESCRIPTIVE NOTES (Type of report and inclusive dates)

Final Report

5. AUTHOR(S) (First name, middle initial, last name)

Joseph Velletri, Robert Spring, James Wagoner, Henry Gignilliat

6. REPORT DATE	7a. TOTAL NO. OF PAGES	7b. NO. OF REFS
December 1968	86	26

8a. CONTRACT OR GRANT NO.	9a. ORIGINATOR'S REPORT NUMBER(S)
DACA 31-67-C-0018	
b. PROJECT NO.	TR - 27
c. Subtask 1117C	9b. OTHER REPORT NO(S) (Any other numbers that may be assigned this report)
d.	NRDL TRC-68-69

10. DISTRIBUTION STATEMENT

Distribution of this Document is Unlimited

11. SUPPLEMENTARY NOTES	12. SPONSORING MILITARY ACTIVITY
	Office of the Civil Defense Office of the Secretary of the Army Washington, D. C. 20310

13 ABSTRACT

This report analyzes the results of experiments to determine the effect of interior partitions, apertures and nonuniform walls on the dose rate in a three story structure.

DD FORM 1 NOV 65 1473 (PAGE 1)

S/N 0101-807-6801

UNCLASSIFIED

Security Classification

14. KEY WORDS	LINK A		LINK B		LINK C	
	ROLE	WT	ROLE	WT	ROLE	WT
Radiation Distribution						
Multistory Structure						
Infinite Field of Contamination						
Interior Partitions						
Apertures						
Nonuniform Walls						
Co-60						